# Mg/Ca-temperature and seawater-test chemistry relationships in the shallow-dwelling large benthic foraminifera *Operculina ammonoides*

David Evans[a], Jonathan Erez[b], Shai Oron[c,d], Wolfgang Müller[a]

[a] *Department of Earth Sciences, Royal Holloway University of London, Egham, TW20 0EX, UK*
[b] *Earth Science Institute, The Hebrew University of Jerusalem, Israel*
[c] *Department of Geological and Environmental Sciences, Ben-Gurion University of the Negev, Beer-Sheva, Israel*
[d] *The Interuniversity Institute for Marine Sciences (IUI), Eilat, Israel*

---

**Abstract**

The foraminifera Mg/Ca palaeothermometer contributes significantly to our understanding of palaeoceanic temperature variation. However, since seawater Mg/Ca has undergone large secular variation and the relationship between seawater and test Mg/Ca has not been calibrated in detail for any species with a substantial fossil record, it is only possible to assess relative temperature changes in pre-Pleistocene fossil samples. In order to establish the basis of accurate quantitative Mg/Ca-derived deep-time temperature reconstructions, we have calibrated the relationship between test Mg/Ca, seawater chemistry and temperature in laboratory cultures of the shallow-dwelling large benthic species *Operculina ammonoides*. *Operculina* has a fossil range extending back to the early Paleogene and is the nearest living relative of the abundant genus *Nummulites*. We find a temperature sensitivity of 1.7%°C$^{-1}$ and a linear relationship between test and seawater Mg/Ca ($Mg/Ca_{sw}$) with m = -1.9×10$^{-3}$, within error of the equivalent slope for inorganic calcite. The higher test Mg/Ca of *O. ammonoides* compared to inorganic calcite may be explained by an elevated pH of the calcifying fluid, implying that these foraminifera do not modify

the Mg/Ca ratio of the seawater from which they calcify, differentiating them in this respect from most other perforate foraminifera. Applying these calibrations to previously published fossil data results in palaeo-Mg/$Ca_{sw}$ reconstruction consistent with independent proxy evidence. Furthermore, our data enable accurate absolute palaeotemperature reconstructions if Mg/$Ca_{sw}$ is constrained by another technique (e.g. ridge flank vein carbonate; fluid inclusions). Finally, we examine Li, Na, Sr and Ba incorporation into the test of *O. ammonoides* and discuss the control exerted by temperature, seawater chemistry, saturation state and growth rate on these emerging proxies.

*Keywords:* Mg/Ca, *Operculina*, *Nummulites*, large benthic foraminifera, palaeotemperature, seawater Mg/Ca

---

## 1. Introduction

The Mg/Ca thermometer is an established palaeoclimatic tool and provides one of the most accurate quantitative techniques in Pleistocene-Holocene ocean temperature reconstruction. Notwithstanding the wealth of information on the climate system gained from the such studies, many of the most interesting intervals with respect to understanding the controls on Earth system sensitivity lie further back in time (Haywood et al., 2011). Since the initial development of the foraminifera Mg/Ca temperature proxy (Rosenthal et al., 1997; Nürnberg et al., 1996), many more species have been investigated and it is now well known that modern foraminifera exhibit a wide range of Mg/Ca ratios that are controlled by calcification physiology as well as temperature (summarised in Bentov & Erez, 2006).

The Mg/Ca palaeothermometer has been applied throughout the Cenozoic (e.g. Lear et al., 2000), although it is now clear that there are fundamental complications with the use of this proxy deeper in geological time, on top of the so-called

'vital effects' which introduce unknown error when applying calibrations to extinct foraminifera. This is principally because the dependence of test Mg/Ca ($Mg/Ca_{test}$) on seawater Mg/Ca ($Mg/Ca_{sw}$) is both non-linear and poorly known for all species abundant in the fossil record (see Evans & Müller, 2012, for an overview). Furthermore, the highest resolution $Mg/Ca_{sw}$ data available (Fantle & DePaolo, 2006) suggest a significant rise ($\sim 2\times$) over the last 4 Ma, implying that even poorly-corrected or uncorrected Mg/Ca data from the Pliocene Warm Period may result in inaccurate palaeotemperature estimates. In order for fossil foraminifera Mg/Ca data to yield accurate absolute temperature reconstruction, both a Mg/Ca-temperature and a $Mg/Ca_{test}$-$Mg/Ca_{sw}$ calibration is required, along with knowledge of $Mg/Ca_{sw}$ for the time of interest. As far as we are aware, this has not yet been achieved for any species. Here, we focus on *Operculina ammonoides* (Family: Nummulitidae), a species closely related to both *Heterostegina depressa* for which a trace element study has been performed (Raitzsch et al., 2010), and the genus *Nummulites* (within the same sub-family) which were widespread throughout the Paleogene (sub)tropics to the extent that they are the principal component of some shallow water carbonates (e.g. Guido et al., 2011). Because of the abundance of nummulitids in the fossil record they represent an under-utilised early-mid Cenozoic palaeoclimate archive.

*Operculina* are symbiont-bearing, shallow-dwelling benthic foraminifera with a peak abundance-depth range comparable to surface-dwelling planktic foraminifera (Evans et al., 2013, and references therein). The hyaline (glassy) appearance of the test is the result of the non-random orientation of the calcite crystals. Chambers are perforate and lamellar; calcite is mineralised each side of an organic matrix with the addition of a new layer to the entire outer test every time a new chamber is deposited (Reiss, 1958). Previous analyses of a number of fossil and recent non-cultured nummulitids have shown that the alkali earth metal distribution coefficients

and their response to temperature and seawater chemistry variation are within error, therefore calibrations based on extant species can therefore be applied to other species within this family in the fossil record (Evans et al., 2013). In order to facilitate comparison to previous work (Raitzsch et al., 2010; Evans & Müller, 2013; Evans et al., 2013) and because different parts of the test have subtly different X/Ca ratios, we focus our geochemical measurements on the marginal cord, the thickened test margin which plays an important reproductive and interchamber cytoplasm transport role.

In order to (1) investigate the controls on trace element incorporation in these LBF, (2) provide the basis of more accurate Mg/Ca-based deep-time (pre-Pleistocene) temperature reconstruction and (3) place constraints on the nummulitid biomineralisation mechanism, we present the first coupled temperature-seawater chemistry-test chemistry calibration for a foraminifera. Whilst we present spatially-resolved data for a suite of commonly analysed elements measured by laser-ablation ICPMS, we focus on the Mg/Ca ratio of foraminiferal calcite because of its potential for palaeoclimate reconstruction and the importance of understanding Mg incorporation for the assessment of biomineralisation models.

## 2. Materials and methods

### *2.1. Culture*

All culturing work was carried out at the Institute of Earth Sciences, The Hebrew University of Jerusalem. *O. ammonoides* were collected from the sediment surface from the northernmost Gulf of Eilat (north beach, Eilat) in May 2012 at a depth of 10-15 m. Water temperature at the time of collection was 22°C. *O. ammonoides* were by far the most abundant organism in the sediment and were sampled from

the 1.0-1.3 mm size fraction. Live foraminifera were identified as being those which climbed container walls. Twelve groups of 50 foraminifera were isolated and placed into 130 ml glass-stoppered conical flasks. Seawater collected from the Gulf of Eilat was used as the basis for all culture reservoirs. Seawater was sampled upon preparation of every new reservoir and cumulative samples of water from the flasks were collected at a rate of 1 ml $day^{-1}$ in order to assess potential water chemistry modification by the foraminifera. The water in each flask was completely replaced every second day, after which the cultures were sealed with Parafilm to prevent salinity modification through evaporation. The different cultures were distributed into water baths according to the requirements of each experiment. Water baths were simultaneously cooled and heated to maintain a temperature within $\pm 0.3$°C of the desired value. Temperature and light measurements were performed twice per day for each water bath. Foraminifera were fed every 1-2 weeks with the diatom *Phaeodactylum tricornutum*. Occasional algal growth on some foraminifera, associated with a sharp decrease in calcification rate, was removed by individual specimen cleaning with a fine paint brush.

Growth rate was monitored by measuring the alkalinity of the individual flasks every second day using a Metrohm 716 DMS titrino. All measurements were duplicated and a third replicate sample was analysed if the difference between them was greater than 8 $\mu$Eq $l^{-1}$. Accuracy was assessed by weekly analysis of the Scripps Institute of Oceanography reference seawater (batch 109). Long term data reproducibility assessed over a two month period was $\pm 11$ $\mu$Eq $l^{-1}$.

All reservoirs were spiked with 0.15 $\mu$M $BaCl_2$ to provide a compositional marker of calcite grown in culture. Ba was chosen because foraminifera Ba/Ca relates linearly to seawater Ba/Ca in planktic species with minor secondary controls (e.g. Lea & Spero, 1992; Hönisch et al., 2011), enabling cultured material to be unambiguously

identified via LA-ICPMS whilst simultaneously analysing proxy (trace) elements. The 0.15 $\mu$M spike used here results in seawater with a Ba/Ca ratio of 17.6 $\mu$mol mol$^{-1}$, $\sim$3 times greater than Gulf of Eilat seawater at the time of foraminifera collection (6.0 $\mu$mol mol$^{-1}$). Cultures at 22.5 and 25.5°C and all those in variable $Mg/Ca_{sw}$ ratios were also labelled with calcein at a concentration of 40 $\mu$M during the first 48 hours of the experimental period.

All cultures were located in the same place and therefore had similar lighting conditions with the exception of those grown at 25.5°C, which were located near a window and were exposed to light intensities $\sim$10% lower than that provided by the artificial laboratory lights. Cultures grown at 27°C were moved to this location (with a greater proportion of natural light) on day 40 of the experiment in order to make room for the 22.5°C water bath.

### *2.1.1. Experiment DE1: Temperature variable, constant seawater chemistry*

To investigate the control of temperature on trace element incorporation, six water baths were prepared in the range 19-27°C. Foraminifera cultured at 19, 21, 24 and 27°C were grown for two months in duplicate cultures, those at 22.5 and 25.5°C were started one month later. There were insufficient remaining foraminifera to duplicate these latter experiments. An attempt to culture *O. ammonoides* at 18°C was unsuccessful, resulting in net dissolution. Reservoir water for all of these cultures was unmodified Gulf of Eilat seawater (table 1).

### *2.1.2. Experiment DE2: Variable seawater Mg/Ca, constant temperature*

The effect of varying $Mg/Ca_{sw}$ on $Mg/Ca_{test}$ in *O. ammonoides* was investigated by culturing foraminifera at five different $Mg/Ca_{sw}$ ratios in the range 2-7 mol mol$^{-1}$ (present-day seawater has $Mg/Ca_{sw}$ = 5.2 mol mol$^{-1}$). We found that this species ceases to calcify in response to sudden changes in seawater chemistry and therefore

had to be gradually acclimatised in order to precipitate $CaCO_3$ in seawater with Mg/Ca<4. A rate of $Mg/Ca_{sw}$ decrease of 0.5 mol $mol^{-1}$ $day^{-1}$ ensured the survival and growth of most foraminifera at 2 mol $mol^{-1}$. Attempts to culture these foraminifera at both 1 and 1.5 mol $mol^{-1}$ were not successful, resulting in growth cessation and the retraction of pseudopods. Modified seawater was prepared by mixing Gulf of Eilat seawater with artificial seawater prepared without Mg following the recipe of Millero (1996), with the exception of the seawater with Mg/Ca = 7 mol $mol^{-1}$ which was made by spiking natural seawater with 20 mM $MgCl_2$. Seawater [Ca] was invariant between all experiments. Salinity was adjusted to 37‰ using a combination of distilled water and NaCl. Alkalinity was increased to that in the Gulf of Eilat at collection via addition of $NaHCO_3$. Individual reservoir characteristics are summarised in table 1.

### *2.2. Analytical chemistry*

#### *2.2.1. Laser ablation*

Prior to LA-ICPMS analysis, organic material was removed from the foraminifera by oxidisation in 10% NaOCl for eight hours. Following this, the foraminifera were ultrasonicated for two minutes, rinsed twice with deionised water, ultrasonicated for one minute in deionised water, rinsed and then left to dry in a class 100 laminar flow air hood overnight. All foraminifera were analysed using the RESOlution M-50 prototype 193 nm ArF laser-ablation system at Royal Holloway, coupled to an Agilent 7500ce ICPMS (Müller et al., 2009). In order to analyse the marginal cord without sectioning (which risks destroying the final chambers), foraminifera were mounted vertically in the ablation cell by pressing individual foraminifera into a pressure-sensitive adhesive such that the marginal cord of the final chambers is perpendicular to and coincides precisely with the laser focal plane, facilitating analysis

by slow depth-profiling (drilling). Given the curved outer surface of the foraminifera we analysed only the final 3-5 chambers in order to remain within the laser focal plane. Because $^{55}$Mn is an isotope of interest, but suffers from $^{40}$Ar$^{15}$N interference, $H_2$ was used instead of $N_2$ as the additional diatomic gas, added downstream of the ablation cell. Depth-profiling analyses were carried out using a 44 $\mu$m spot and a repetition rate of 2 Hz at a fluence of $\sim$3 J cm$^{-1}$. Because it is necessary to use a signal-smoothing device to avoid 'beating' at low repetition rates (Müller et al., 2009), 99% signal washout time was $\sim$3 s, giving an effective spatial depth resolution of $\sim$0.5 $\mu$m. ICPMS setup and data reduction was performed as previously described (Müller et al., 2009; Evans et al., 2013) with the exception of the Ar carrier gas flow rate, increased to $\sim$600 ml min$^{-1}$ as $H_2$ instead of $N_2$ was used as the additional diatomic gas. Isotopes analysed were $^{7}$Li, $^{11}$B, $^{24}$Mg, $^{25}$Mg, $^{27}$Al, $^{43}$Ca, $^{55}$Mn, $^{66}$Zn, $^{88}$Sr, $^{89}$Y, $^{137}$Ba, $^{138}$Ba, $^{146}$Nd and $^{238}$U. NIST612 was used as an external (calibration) standard, with the exception of B and Ba which were calibrated to NIST610 and Mg which was calibrated to the MPI-DING komatiite glass GOR132 (Jochum et al., 2006). With the exception of Mg/Ca, the calibration standard was chosen by assessing GOR128 and GOR132 accuracy using both NIST glasses. GOR132 was used to calibrate Mg data as both NIST glasses exhibit Mg heterogeneity (both NIST glasses have Mg 2SD of $\sim$7% compared to 0.9% for GOR132) which is large enough to enlarge errors and bias data if too few NIST analyses are performed to obtain a representative mean Mg intensity-concentration relationship.

Accuracy was assessed by calibrating 36 analyses of the MPI-DING glasses GOR132 and GOR128 to both NIST610 and NIST612. In all cases accuracy for X/Ca ratios discussed hereafter is better than 5%, with the exception of Li/Ca (12.4%) and Ba/Ca (7.4%). These values are based on the standard combination that resulted in the smallest accuracy (with the constraint that the calibration standard must be

the same as that used for the foraminifera), as larger offsets were assumed to be the result of a combination of error in the reported value of the NIST or MPI glass, or heterogeneity in either the calibration standard or that treated as an unknown. A detailed assessment of the data quality is given in the supplementary material. It was not possible to assess precision by repeat analysis of the foraminifera, as they are heterogeneous on a scale smaller than the diameter of the laser beam. Instead we report 2SD of the komatiite glasses GOR132 and GOR128. As before, the smallest precision value based on all possible NIST-MPI combinations was chosen as larger spreads likely indicate standard heterogeneity. Precision for all X/Ca ratios was better than 10% with the exception of Al/Ca and Sr/Ca (<5%) and Ba/Ca (13.7%); see the supplementary material for a more comprehensive analysis. Whilst these precision data give an indication of the error that should be applied to an individual analysis, we do not propagate precision into error bars where the mean of a large number of analyses is under consideration.

### *2.2.2. Solution ICPMS*

Seawater samples were analysed using an Agilent 7500cx ICPMS at the NERC Isotope Geosciences Laboratory (Keyworth, UK). Samples were acidified to 1% $HNO_3$ and 0.5% HCl and analysed at 25× dilution with the exception of Mg and Ca which were analysed at 50× dilution. Intensity/internal standard ratios were calibrated against three trace element (1, 10, 100 ppb) and three major element solutions. A pre-run calibration blank was used to define the y-intercept of the calibration lines. All samples were analysed twice, both with and without He (5.5 ml $min^{-1}$) in the collision/reaction cell; each reported m/z was monitored only in the most appropriate gas mode (see the supplementary material).

Accuracy and precision were assessed either by triplicate analysis of the seawater

standard NASS-4 and the riverine water standard SLRS-2, or using the analyses of the experiment seawater reservoirs in the case of Mg/Ca, Na/Ca and Sr/Ca (where these ratios were not modified through experimental design) as (1) these elements behave conservatively in the ocean and (2) there is no significant freshwater input to the Gulf of Eilat, therefore we expect to find ratios equivalent to the bulk ocean. It was not possible to assess accuracy for Li or B as no standards were analysed with certified values for these elements, in these cases errors are based only on NASS-4 precision. Similarly, accuracy derived from freshwater standards (Na, Ba, U) should be applied to seawater analyses with caution, although we nevertheless do so in the absence of a certified seawater standard and note that these data are likely to overestimate error because the ICPMS was configured to optimise data for high-Na samples with a very different matrix to riverine water. NASS-4 was diluted in the same way as the seawater samples, SLRS-2 was not diluted prior to analysis. All seawater Al, Mn, Zn, Y and REE data are below the LOD. Mg/Ca and Sr/Ca accuracy (%) $\pm$ precision (RSD) derived from all analyses of Gulf of Eilat seawater (reservoir and cumulative water samples, n = 14) compared to the Mg/Ca value of Lebel & Poisson (1976) and the mean Sr/Ca value of de Villiers (1999) are 3.5$\pm$1.5 and 2.5$\pm$4.8% respectively. Na/Ca, Ba/Ca and U/Ca accuracy$\pm$precision are 3.6$\pm$9.6, 10.2$\pm$4.6 and 2.9$\pm$6.5% respectively, based on triplicate SLRS-2 analyses (see the supplementary material).

The major and trace element concentrations of the cumulative water samples are within error of the equivalent reservoir. Given that the reservoir samples have less potential for contamination (cumulative samples were opened every second day) we base our calculation of distribution coefficients on the reservoir seawater analyses.

### *2.3. Carbonate chemistry*

Carbonate chemistry parameters not directly measured ($\Omega_{\text{calcite}}$, $[CO_3^{2-}]$) were calculated from alkalinity and pH using the co2sys Matlab function (Lewis & Wallace, 2006) and the same set of constants as Raitzsch et al. (2010). For the purpose of assessing the relationship between carbonate chemistry and trace element distribution coefficients we use the mean difference between the cumulative water samples (2 ml from the cultures was collected every second day when the water in the flasks was replenished) and the reservoir. It was necessary to replace the water every two days in this way as the foraminifera were cultured in a closed system and were present in sufficient number to modify the chemistry of seawater from which they calcified. For example, within the variable temperature experiment the pH of the cumulative water samples was 0.08 lower on average than that of the reservoir water, translating to a carbonate ion concentration reduction of $\sim$40 $\mu$M.

## 3. Results

Compositional data along with calculated physiological and carbonate chemistry parameters are shown in tables 2 and 3.

### *3.1. Calcification*

#### *3.1.1. Calcification rate*

Cumulative average growth curves derived from alkalinity measurements for each of the individual cultures are shown in figure 1. Cultures kept at 24°C grew consistently faster than all others, with the exception of culture DE1-7 (27°C) which underwent an increase in growth rate after it was moved on day 40 to an area with $\sim$10% lower mean light intensity and a greater proportion of natural light. No geochemical differences were observed between calcite precipitated prior to and after this

time, including elements such as Sr which are known to be growth rate dependent in at least some planktic foraminifera (Kisakürek et al., 2008); see the supplementary material. A probable explanation is that individual specimen growth rate did not change, but rather individuals that were not previously calcifying began to form new chambers when moved to an area of lower light intensity, given that each culture contained 50 individuals and calcification rates represent an average of that number of individuals. A change in the number of calcifying individuals rather than the overall calcification rate can also explain why no increase in growth rate was observed in the repeat culture at this temperature (figure 1). There is no evidence that moving this culture resulted in identifiable geochemical bias.

Light intensity for all cultures was virtually identical (aside from the previously mentioned exceptions), therefore this cannot explain the remainder of the inter-culture growth rate variation. For cultures of equivalent lighting conditions, those at 19°C (DE1-1 and -2) and 27°C (DE1-7 and -8) grew at 50% of the rate of those at 24°C. It is unsurprising that the cultures characterised by the highest growth rates were those grown under conditions most similar to that of the mean annual Gulf of Eilat temperature at the foraminifera collection depth, although some of the observed variation may be a result of acclimatisation to the new conditions. Therefore, it is possible that culture growth rates do not translate in any meaningful way to natural changes in response to long-term environmental change. Duplicate cultures grown at the same temperature exhibit large differences in calcification rate despite all other conditions being equal. Repeat cultures show a difference in cumulative calcification of up to 360%, although those at 24°C are within error of each other. Because each experiment consisted of 50 foraminifera, these substantial differences are unlikely to result from random variation in the initial population and may suggest that these foraminifera are capable of influencing overall group calcification rates. All

cultures in the variable seawater chemistry experiment, including that with modern $Mg/Ca_{sw}$, grew at a rate ~50% of those at the same temperature (24°C) in the Mg/Ca-temperature experiment. Given the variation in growth rate between repeat cultures in unmodified seawater, it is not possible to assess whether this was because of the modified seawater chemistry.

Figure 1C shows the relationship between mean $\Omega_{calcite}$ (the average between the reservoir and cumulative water $\Omega$ for each culture) and growth rate, normalised by multiplying by the ratio of the number of foraminifera analysed to the number of foraminifera that precipitated at least one chamber during the culture period (see table 2). Calcifying foraminifera were identified as those that precipitated at least one chamber with elevated Ba/Ca (see section 3.1.2). Normalised growth rate is positively correlated with mean culture $\Omega$ for the variable temperature experiment, although cultures that calcified very slowly (DE1-4 and all DE2) do not fit this trend.

### *3.1.2. Identifying cultured calcite*

Calcein labelling and modifying seawater [Ba] are both effective methods of identifying new chambers in cultured foraminifera. Newly formed chambers in specimens from cultures that were labelled with calcein (table 1) are easily identifiable (figure 2). The majority of foraminifera precipitated at least one new chamber during the labelling period (figure 2A, C, D) from calcein-spiked vacuolised seawater, producing highly fluorescent calcite. Preceding chambers are weekly fluorescent because these foraminifera add a layer of calcite to their entire outer surface when a new chamber is formed (e.g. Erez, 2003), enabling newly formed calcite to be identified in foraminifera which did not calcify during the labelling period because new chambers are non-fluorescent (figure 2B).

Examples of laser-ablation profiles of calcifying and non-calcifying specimens are

shown in figure 3C and D respectively. These analyses demonstrate that *O. ammonoides* adds a new layer of calcite to the existing marginal cord during chamber formation, as some depth profiles show a decrease in both Mg/Ca and Ba/Ca representing the transition from calcite precipitated in culture to pre-existing calcite. The Ba/Ca-Mg/Ca pattern of the specimen shown in figure 3C is a result of the lower temperature of the Gulf of Eilat in which these foraminifera originally calcified (lower test Mg/Ca) compared to the culture temperature (27°C), unambiguously identifiable using Ba/Ca. The specimen shown in figure 3D is characterised by lower Mg/Ca and Ba/Ca because it precipitated the analysed calcite prior to collection at ~22°C, and in seawater that was not spiked with $BaCl_2$. Based on such profiles, all laser-ablation ICPMS data were categorised into representing new or existing calcite by setting a test Ba/Ca cut-off point at 9 $\mu$mol mol$^{-1}$ below which it was judged that the analysed material was entirely or partially composed of calcite precipitated prior to culture. Furthermore, analyses characterised by Mg/Ca and Ba/Ca 2RSD >20% were also excluded on the basis that these were likely to partly consist of calcite grown at a temperature other than that of the culture (chamber f-4, figure 3C Mg/Ca RSD = 21.4% compared to 13.8% for the final chamber which also has consistently high Ba/Ca). These data therefore enable the non-qualitative exclusion of analyses which represent a mix of calcite precipitated before and after the start of the experiment.

All analyses from the two extremes of the variable temperature experiment are shown in figure 3E and F in order to further demonstrate the effectiveness of this technique. Each data point in these plots does not necessarily represent a single chamber, as it is possible to fit more than one ablation spot on the marginal cord within a single chamber (figure 3B). Analyses characterised by relatively low Ba/Ca ratios (4-6 $\mu$mol mol$^{-1}$) have Mg/Ca ratios within the range of control specimens that

were collected at the same time as cultured individuals but immediately washed and dried (Evans et al., 2013), implying that this calcite was formed prior to the start of the experiment. These data points are distinct in Mg-Ba space (i.e. there is no continuum) from those with high Ba/Ca ratios and Mg/Ca offset from that of non-cultured specimens. Within this subset, analyses derived from individuals cultured at 19°C have lower Mg/Ca than the control group, whereas the opposite is the case for those cultured at 27°C. This is consistent with the estimated growth temperature of these foraminifera prior to collection (early May), which remains at $\sim$22$\pm$1°C from November to April. Therefore calcite precipitated prior to culture (with low Ba/Ca) should have an intermediate Mg/Ca ratio between the two extremes of the temperature experiment, as observed.

### *3.2. Trace element chemistry*

#### *3.2.1. Mg/Ca-temperature calibration*

The results of our temperature calibration experiment define a Mg/Ca sensitivity within error of the gradient given by a comparative field calibration of the same species (Evans et al., 2013), see figure 4. Linear and exponential regressions describe the data equally well. We present both here to facilitate comparison to previous work and because the reconstruction of relative temperature shifts in fossil samples is more complex with linear Mg/Ca-temperature regressions (see Evans et al. (2013) and supplementary material). Based on the culture data presented here, the relationship between Mg/Ca and temperature for *O. ammonoides* is:

$$ln(\mathrm{Mg/Ca}) = 0.0181 \pm 0.0026 \times T + 4.52 \pm 0.06 \quad (1)$$

Or in linear form:

$$\mathrm{Mg/Ca} = 2.55 \pm 0.39 \times T + 81.7 \pm 9.0 \quad (2)$$

Combining these laboratory culture data with the *O. ammonoides* field samples of Evans et al. (2013) results in the following exponential and linear relationships:

$$ln(\mathrm{Mg/Ca}) = 0.0168 \pm 0.0018 \times T + 4.55 \pm 0.05 \quad (3)$$

$$\mathrm{Mg/Ca} = 2.41 \pm 0.24 \times T + 84.2 \pm 6.1 \quad (4)$$

All regression errors are ±2SD. Mg/Ca error bars in figure 4 are ±2SE of the mean of all analyses for a given culture, effectively comparable to calibrations based on analyses of multiple dissolved foraminifera analysed by solution ICP-MS/AES. Mg/Ca data from duplicate cultures were pooled as no significant offset was observed (table 3). For comparison, data from the small, shallow-dwelling, hyaline benthic foraminifera *Planoglabratella opercularis* (Toyofuku et al., 2000) are also shown in figure 4. This species has a slope and intercept (2.23, 89.6) within error of our *O. ammonoides* calibration, although the species are not closely related.

The Gulf of Eilat seawater used for the culture calibration has a salinity of 40.65‰, up to 8‰ higher than the sample sites of Evans et al. (2013) which were predominantly within SE Asia and characterised by salinities of 33-36‰, yet the individual calibrations in figure 4 define Mg/Ca-temperature relationships that are virtually identical. Data from two other species within the Nummulitidae family, *O. complanata* (Evans et al., 2013) and *Heterostegina depressa* (Raitzsch et al., 2010), the latter cultured at a salinity of 36‰, fall on the same line. Therefore, there is no evidence that this large salinity difference between sample sites/cultures has any control on *O. ammonoides* Mg/Ca; the offset between foraminifera living at

the same temperature but different salinity is always smaller than the error in the laser-ablation measurements.

*3.2.2. Test-seawater Mg/Ca relationship*

The relationship between $Mg/Ca_{test}$, $D_{Mg}$ ($[Mg/Ca_{test}]/[Mg/Ca_{sw}]$) and $Mg/Ca_{sw}$ is shown in figure 5. $D_{Mg}$ varies linearly with $Mg/Ca_{sw}$:

$$D_{Mg} = -0.00190 \pm 0.00034 \times Mg/Ca_{sw} + 0.0366 \pm 0.0016 \quad (5)$$

Manipulating this calibration by multiplying through by $Mg/Ca_{sw}$ results in a $2^{nd}$ order polynomial relationship between $Mg/Ca_{sw}$ and $Mg/Ca_{test}$ which passes through the origin, because $[D_{Mg} = a \times Mg/Ca_{sw} + b] \times Mg/Ca_{sw}$ is equivalent to $Mg/Ca_{test} = a \times (Mg/Ca_{sw})^2 + b \times Mg/Ca_{sw}$. Therefore, at 24°C:

$$Mg/Ca_{test} = -1.98 \pm 0.39 \times (Mg/Ca_{sw})^2 + 37.02 \pm 2.16 \times Mg/Ca_{sw} \quad (6)$$

Where $Mg/Ca_{test}$ is expressed in mmol $mol^{-1}$. The data of Raitzsch et al. (2010) derived from *H. depressa*, are also shown for comparison in figure 5C.

Previous studies that have examined the shape of the relationship between fluid and calcite Mg/Ca in both foraminiferal and inorganic calcite have argued that this relationship is best described by a power regression (Ries, 2004; De Choudens-Sánchez & González, 2009; Hasiuk & Lohmann, 2010; Evans & Müller, 2012). The linear relationship between $D_{Mg}$ and $Mg/Ca_{sw}$ reported here, which implies a polynomial relationship between $Mg/Ca_{sw}$-$Mg/Ca_{test}$, is comparable to that derived from inorganic precipitation experiments (Mucci & Morse, 1983) when only data over an equivalent range of $Mg/Ca_{sw}$ values are considered. Whilst all inorganic data (including $Mg/Ca_{sw}$ ratios >8 and <1) are best described by a power relationship between

$D_{Mg}$ and $Mg/Ca_{sw}$ (De Choudens-Sánchez & González, 2009; Mucci & Morse, 1983), there is no evidence that Cenozoic seawater was characterised at any point by such ratios and we therefore limit our discussion to calcite precipitated from seawater with Mg/Ca between 1-8 mol $mol^{-1}$, for which a linear $D_{Mg}$-$Mg/Ca_{sw}$ regression (and therefore a polynomial $Mg/Ca_{sw}$-$Mg/Ca_{test}$ regression) best describes our data. The regressions defined in equations 5 and 6 should not be extrapolated above $Mg/Ca_{sw}$ = 8 mol $mol^{-1}$, as the vertex of the quadratic $Mg/Ca_{sw}$-$Mg/Ca_{test}$ regression is approached.

To facilitate comparison to previous studies (e.g. Hasiuk & Lohmann, 2010) we also give the equivalent power regressions (these are shown in relation to previous foraminifera calibrations in the supplementary material):

$$Mg/Ca_{test} = 41.4 \times Mg/Ca_{sw}{}^{0.72} \quad (7)$$

$$D_{Mg} = 0.041 \times Mg/Ca_{sw}{}^{-0.28} \quad (8)$$

Which have $R^2$ values of 0.99 and 0.92, the later of which is substantially lower than that for a linear $D_{Mg}$-$Mg/Ca_{sw}$ regression (0.99, figure 5).

*3.2.3. Controls on other proxy trace element incorporation in nummulitid calcite*

Both calcite and seawater were also analysed for Li, Na, Sr and Ba, as these are either established or emerging proxy systems in other species and important for biomineralisation models. The cultures grown at different temperatures enable this potential control on other trace element distribution coefficients to be investigated, whilst the artificial-natural seawater mixes of the variable $Mg/Ca_{sw}$ experiments are characterised by variable seawater Li-Na-Sr-Ba/Ca ratios. Specifically, the artificial seawater has ∼3× lower Li/Ca whilst Na/Ca and Sr/Ca were ∼15% higher than Gulf

of Eilat seawater. The relationships described in this section should be viewed with caution given that some variables, namely growth rate and foraminifera-mediated saturation state changes, were beyond our control and may simultaneously affect proxy incorporation. This complication is not unique to our dataset, although our monitoring of growth rate and carbonate chemistry do enable preliminary interpretations to be drawn.

Test Li/Ca shows a weak negative correlation with temperature ($R^2 = 0.48$, figure 6A) with a gradient similar to *Cibicidoides pachyderma* corrected for saturation state Lear et al. (2010); Bryan & Marchitto (2008). There is a strong positive relationship between seawater and test Li/Ca ($R^2 = 0.98$) with a slope ∼30 times steeper than both the Li/Ca-temperature relationship observed here and the Li/Ca-$\Delta CO_3^{2-}$ relationship observed by Bryan & Marchitto (2008). Saturation state and Li/Ca are weakly negatively correlated in the variable seawater chemistry experiment ($R^2 = 0.22$) whereas the weak negative relationship between Li/Ca and Ω in the variable temperature experiment (figure 6C) is not significant because it is an artefact of the Li/Ca-temperature relationship, given that temperature exerts a control on Ω. Growth rate is strongly correlated with Li/Ca and Ω in experiment DE2 which is not supported by data from experiment DE1, this is likely to be an artefact of lower growth rates in the cultures with seawater chemistry most different from natural.

Na/Ca is weakly positively correlated with culture temperature ($R^2 = 0.72$) and uncorrelated with seawater Na/Ca in these experiments (figure 6E). The curved relationship with $Na/Ca_{max}$ at ∼25°C is similar in appearance to the shape of the temperature-growth rate curve for these cultures suggesting that growth rate may be the principal reason for $Na/Ca_{test}$ variation in our experiments. If the culture with the lowest growth rate is considered to be an outlier then growth rate and Na/Ca are moderately well correlated ($R^2 = 0.63$, figure 6H), based on the combination of both

experiments. Moreover, the data from the variable seawater chemistry experiment show a very strong correlation with growth rate, despite constant temperature and broadly equivalent $Na/Ca_{sw}$. The salient point is that there are significant controls on Na/Ca incorporation in *O. ammonoides* other than salinity, which varies by only 1‰ between the cultures in experiment DE2 and yet these cultures show a 4 mmol $mol^{-1}$ ($\pm$10%) shift in Na/Ca. An extended discussion of our *O. ammonoides* Na/Ca data in the context of other foraminifera is given in section 4.3 and the supplementary material, with particular regard to our analytical and cleaning protocols. We demonstrate that the Na/Ca ratios of *O. ammonoides*, $\sim$2$\times$ higher than some other foraminifera, are not artefacts of the sample preparation process.

There is no evidence for a relationship between $Sr/Ca_{test}$ and temperature, $Sr/Ca_{sw}$ (figure 6N) or growth rate control based on our experiments in this foraminifera. See below and section 4.3 for an explanation of the lack of a test-seawater Sr/Ca relationship. Similarly, there is no statistically significant correlation between $\Omega$ and $Sr/Ca_{test}$ (figure 6O).

Ba/Ca is negatively correlated with temperature ($R^2 = 0.87$, figure 6Q), characterised by a 0.17 $\mu$mol $mol^{-1}$ decrease $°C^{-1}$. Similarly to the Na/Ca data, the cultures at 27°C are offset from the trend defined by the rest of the experiments, although to a lesser extent. Our $Ba/Ca_{test}$-$Ba/Ca_{sw}$ data confirm the linear relationship observed in planktic foraminifera (Hönisch et al., 2011) although the gradient for this species is more than four times steeper than that of *Orbulina universa*. The culture data presented here, along with Ba/Ca measurements of non-cultured *O. ammonoides* from both the Gulf of Eilat and several samples from southeast Asia (Evans et al., 2013), define the following test-seawater Ba/Ca relationship ($R^2 = 0.95$):

$$Ba/Ca_{test} = 0.62 \pm 0.003 \times Ba/Ca_{sw} \quad (9)$$

The Ba/Ca data from the variable seawater chemistry experiment alone define a steeper slope (m = 1.16) compared to equation 9. Furthermore, the cultures with the highest and lowest $Ba/Ca_{sw}$ are offset from the line defined by equation 9 to an extent greater than that which may be reasonably expected based on the combined analytical errors for the seawater and calcite data. This implies that Ba/Ca has a secondary control other than temperature, and/or that the test-seawater relationship is more appropriately described by an exponential relationship ($R^2$ = 0.97 based on all of the data shown in figure 6R). The data derived from experiment DE2 are very strongly correlated with $\Omega$ (figure 6S) although this is an artefact of the $Ba/Ca_{sw}$ correlation with mean culture $\Omega$. There is unlikely to be a causal relationship between these parameters, although it may not be coincidental that the extent to which the foraminifera modified the saturation state of the seawater is well correlated with the proportion of Eilat seawater in these artificial:natural seawater mixtures. The correlation between $Ba/Ca_{test}$ and growth rate for experiment DE2 is likely an artefact for similar reasons, the variable temperature experiment does not support this relationship.

As well as the multiple dependent variables that complicate the interpretation of the $X/Ca_{test}$-growth rate-$\Omega$ relationships (figure 6), these data should also be viewed with the caveat that trace element distribution coefficients may influence each other. For example Sr/Ca incorporation in inorganic calcite is dependent to some extent on calcite Mg/Ca (Mucci & Morse, 1983). Figure 6 implies that there is no significant temperature, growth rate or saturation state control on Sr-incorporation in *O. ammonoides*. In particular, the lack of correlation between seawater-test Sr/Ca is superficially surprising given that previous work on *H. depressa* have shown that these parameters are highly dependant. Following Mucci & Morse (1983), figure 7A shows the relationship between test Mg/Ca and $D_{Sr}$. The *O. ammonoides* $D_{Sr}$-

$Mg/Ca_{test}$ relationship is within error of that for inorganic calcite (see figure 7A for regression coefficients), demonstrating that $Mg/Ca_{test}$ is the dominant control on $D_{Sr}$ in our experiments. This is because the $Mg/Ca_{test}$ ratio is far more variable between cultures than $Sr/Ca_{sw}$, which is why we observe no test-seawater Sr/Ca relationship. The data of Raitzsch et al. (2010) for *H. depressa* also broadly conform to both those presented here and to inorganic calcite, although the $Mg/Ca_{test}$-$D_{Sr}$ slope is far steeper for *H. depressa* alone (m = 5.13 cf. 0.91 for inorganic calcite). A similar plot of $D_{Na}$-$Mg/Ca_{calcite}$ (figure 7B) shows that for a wide range of foraminiferal and inorganic calcites (Ishikawa & Ichikuni (1984); Okumura & Kitano (1986); Wit et al. (2013), this study and our unpublished laser-ablation data for *Amphistegina lobifera*), Na-incorporation is also controlled by the Mg/Ca ratio, with a gradient of $2.94\times10^{-6}$ per 1 mmol $mol^{-1}$ increase in Mg/Ca.

## 4. Discussion

### *4.1. Mg/Ca-derived palaeoreconstruction*

Accurate pre-Pleistocene Mg/Ca palaeothermometry requires a good understanding of the relationship between $Mg/Ca_{sw}$, $Mg/Ca_{test}$ and temperature, as well as an independent estimate of seawater Mg/Ca for the time interval of interest (Evans & Müller, 2012). Given that the majority of proxy and model data show that seawater was characterised by lower Mg/Ca throughout almost all of the Cenozoic compared to the present day (e.g. Coggon et al., 2010; Stanley & Hardie, 1998), Mg/Ca data from fossil material older than a few million years may at best only be used to reconstruct relative changes in temperature. Although previous calibrations between seawater and test Mg/Ca have been carried out at lower than present-day $Mg/Ca_{sw}$ values for *Globigerinoides sacculifer* (Delaney et al., 1985) and two species of *Amphistegina*

(Segev & Erez, 2006), these currently have limited applicability because Delaney et al. (1985) simultaneously varied several experimental parameters and there is no published Mg/Ca-temperature calibration for *Amphistegina*. Here, we show how our data may be used to accurately reconstruct absolute temperature derived from Mg/Ca measurements of pre-Pleistocene foraminifera, when seawater Mg/Ca cannot be assumed to be the same as present day.

The consistency of the Mg/Ca-temperature relationship between the field and laboratory, at different salinities, in seawater with different trace element chemistry, and between species in this family (figure 4) strongly suggests that secondary controls do not exert an influence on $Mg/Ca_{test}$ greater than the magnitude of analytical error. Therefore, equations 3-6 can be applied to fossil nummulitids with confidence, based on the combined data from field and laboratory cultured foraminifera. The data of Toyofuku et al. (2000) show that for a different shallow benthic foraminifera with a similar Mg/Ca-temperature sensitivity and Mg/Ca ratios to *O. ammonoides* (figure 4) salinity also does not significantly affect Mg incorporation, further demonstrating the robustness of Mg/Ca palaeothermometry based on these high-Mg foraminifera in the fossil record.

Following Evans & Müller (2012), coupling equations 4 and 6 defines a surface in temperature-$Mg/Ca_{test}$-$Mg/Ca_{sw}$ space that, given a fossil Mg/Ca measurement, can be used to reconstruct either temperature or $Mg/Ca_{sw}$ if the other parameter is constrained independently (figure 5C):

$$Mg/Ca_{test} = \frac{-1.98 \times (Mg/Ca_{sw}^{t=t})^2 + 37.0 \times Mg/Ca_{sw}^{t=t}}{-1.98 \times (Mg/Ca_{sw}^{t=0})^2 + 37.0 \times Mg/Ca_{sw}^{t=0}} \times 94.8 \exp^{0.0168T} \quad (10)$$

Where t=0 is the present and t=t is some point in the past. Coupling the calibrations in this way assumes that solution Mg/Ca does not alter the exponential

constant of the Mg/Ca-temperature calibration. Whilst the mathematical form of this relationship differs slightly from the methodology described in Evans & Müller (2012) in that it is based on a polynomial rather than a power relationship between $Mg/Ca_{sw}$ and $Mg/Ca_{test}$, using such a relationship does not alter the conclusions of Evans & Müller (2012) because both types of regression produce a convex-up curve that predicts a higher $Mg/Ca_{test}$ at a given $Mg/Ca_{sw}$ compared to the widely held assumption that there is a linear relationship between these two parameters. Therefore, the data we report here support the conclusions of Evans & Müller (2012) and it may be the case that planktic foraminifera and other marine organisms do mediate the calcification process such that a power relationship between test-seawater Mg/Ca most appropriately describes the data. We also stress that the calibrations presented here are consistent with those previously established for inorganic calcite, which indicate that over a very wide range of $Mg/Ca_{sw}$ values (0.25-10 mol $mol^{-1}$) a power relationship best describes the change in $D_{Mg}$ with $Mg/Ca_{sw}$ (De Choudens-Sánchez & González, 2009). However, we fit a linear regression between these parameters as this most parsimoniously describes our data as well as the subset of inorganic calcite data over the range $Mg/Ca_{sw}$ = 1-8 mol $mol^{-1}$.

Equation 10 defines a surface in $Mg/Ca_{sw}$-$Mg/Ca_{test}$-temperature space (figure 5C). Given that it appears that secondary controls on Mg/Ca are within analytical error for this group of foraminifera, the point of intersection of this surface with any two of the three planes defined by a fossil Mg/Ca measurement and a palaeotemperature or $Mg/Ca_{sw}$ reconstruction defines the position of the third. It is not possible to produce an absolute paleotemperature or $Mg/Ca_{sw}$ reconstruction if the shape of this surface is not calibrated in these three dimensions. Applying this coupled calibration to the Eocene (Bartonian) fossil data reported in Evans et al. (2013) yields a reconstructed $Mg/Ca_{sw}$ of 2.38±0.23 mol $mol^{-1}$.

Whilst we provide the basis for the first accurate Mg/Ca-derived palaeotemperatures, considerable further work is required before this palaeothermometer can be accurately applied to samples older than ∼1-2 Ma. Aside from complications resulting from secondary controls on Mg incorporation into foraminiferal calcite (with the exception of the nummulitids), three significant advances are required before this proxy can be widely applied with confidence: (1) the validity of assuming the constancy of the exponential component of a Mg/Ca-temperature calibration must be tested (see the supplementary material for further discussion), (2) an accurate, Ma-resolution Cenozoic $Mg/Ca_{sw}$ record is required and (3) coupled calibrations such as the one presented here are needed for planktic foraminifera widely utilised in ocean sediment cores.

### *4.2. Implications for biomineralisation*

These foraminifera are characterised by test Mg/Ca ratios 10-100 times higher than planktic or deep-benthic foraminifera which typically have Mg/Ca <10 mmol $mol^{-1}$ (e.g. Nürnberg et al., 1996; Lear et al., 2002). Furthermore, the gradient of the relationship between Mg/Ca and temperature for *O. ammonoides* (equations 1-4; ∼1.7%°$C^{-1}$) is much shallower than that for almost all other foraminifera species for which this relationship has been calibrated; planktic foraminifera are typically characterised by Mg/Ca-temperature calibration slopes which increase by more than 7%°$C^{-1}$ (e.g. Kisakürek et al., 2008). Several features of our laboratory culture data suggest that the biomineralisation mechanism of *O. ammonoides* resembles inorganic precipitation from seawater with unmodified elemental chemistry. The gradient of the $D_{Mg}$-$Mg/Ca_{sw}$ calibration is within error of the respective slope for inorganic calcite precipitation (Mucci & Morse, 1983), and the relationship between $D_{Mg}$ and temperature is much closer to that of inorganic calcite than to any other foraminifera

(Oomori et al., 1987), see figure 8. This may suggest that, with the exception of the carbonate chemistry, these foraminifera do not significantly biologically mediate the major and trace element chemistry of the solution in the calcifying space from that of seawater.

Given that foraminifera are known to elevate the pH of the internal seawater vacuoles that arrive to the site of calcification (Bentov et al., 2009), the $D_{Mg}$ offset we observe between *O. ammonoides* and inorganic calcite for a given $Mg/Ca_{sw}$ and temperature may be entirely explained by the biologically-mediated pH elevation during calcite precipitation (figure 8). This is because there is good evidence that pH exerts a control on the $D_{Mg}$ of inorganic calcite (Burton & Walter, 1991) which likely accounts for the offset of our calibration to higher $Mg/Ca_{test}$ ratios at a given seawater Mg/Ca ratio; these authors observed $D_{Mg}$ $\sim$0.006 higher at pH 8.9 compared to precipitates at normal seawater pH. If this hypothesis is correct, it provides further evidence that the calcification mechanism in *O. ammonoides* is not fundamentally different from inorganic precipitation from high-pH seawater. The y-intercept offset between our calibration and that for inorganic calcite provides a rudimentary way of calculating the pH of the calcification site, assuming that this relationship is indeed the case for this foraminifer, given that Burton & Walter (1991) demonstrate that $D_{Mg}$ dependence on pH is linear, and that there is no significant temperature effect on the slope of this relationship. Inorganic calcite $D_{Mg}$-pH gradients vary inconsistently between 6.2-7.7$\times10^{-3}$ over the range 25-45°C but are all within error of each other. Applying these slopes to the *O. ammonoides*-inorganic offset between $D_{Mg}$ and $Mg/Ca_{sw}$ or temperature shown in figure 8 would imply pH at the calcification site elevated 1.1-1.4 units above normal seawater, which is in broad agreement with Bentov et al. (2009) and de Nooijer et al. (2009).

The similarity between the relationship between Mg/Ca-temperature and seawater-

test Mg/Ca in this family and inorganic calcite may suggest a different biomineralisation mechanism to other foraminifera (with the exception of *P. opercularis* which has a similar or identical Mg/Ca-temperature slope to *O. ammonoides* (Toyofuku et al., 2000); figure 4), or at least a greatly reduced or absent role of calcite Mg/Ca manipulation by mitochondrial sequestration or binding with enzymes such as ATP, as suggested for other foraminifera (Bentov & Erez, 2006). It therefore seems possible that these foraminifera calcify by forcing inorganic precipitation from vacuolised seawater with an elevated pH but unmodified Mg-Sr/Ca. In order to precipitate 7 $\mu$g $CaCO_3$ $day^{-1}$ (the maximum observed growth rate) these foraminifera would need to cycle $\sim$14$\times$ their own volume in seawater which seems possible given the size and abundance of large vesicles observed in other large benthic species (e.g. Bentov et al., 2009). Elevating the pH of internal seawater vacuoles is consistent with a carbon concentrating mechanism such as that demonstrated by ter Kuile & Erez (1987) and ter Kuile et al. (1989) using the mechanism suggested by Bentov et al. (2009), whereby the foraminifer elevates the pH of the vacuole enabling diffusion of respiratory $CO_2$ from the surrounding cytoplasm and acidic seawater vesicles, which is necessary because modern seawater has $[Ca^{2+}]$ = 10.2 mM but $[CO_3^{2-}]$ = $\sim$200 $\mu$M. In contrast, it is difficult to explain the high Mg/Ca ratio of the calcite produced by these foraminifera through modification of the concentration of the alkali earth metals in the seawater vacuoles as it would imply that Mg is being added rather than removed. Inorganic precipitation experiments investigating trace element distribution coefficients other than $D_{Mg}$ conducted at elevated pH would test the validity of this model, as would Mg isotope measurements (Pogge von Strandmann, 2008).

The higher Na/Ca ratios of *O. ammonoides* compared to planktic foraminifera (Delaney et al., 1985), a low-Mg benthic foraminifera (Wit et al., 2013) and inorganic precipitates (Ishikawa & Ichikuni, 1984; Okumura & Kitano, 1986) is a direct result

of the higher Mg/Ca ratios of this species (figure 7B). The inorganic precipitates described by (Ishikawa & Ichikuni, 1984; Okumura & Kitano, 1986) are characterised by $D_{Na}$ similar to low-Mg foraminifera because they were precipitated from solutions with very low [Mg]. The relatively high Sr/Ca ratios of these foraminifera compared to other species is a consequence of lattice distortion as a result of their higher Mg concentration, as previously suggested for inorganic calcite (Mucci & Morse, 1983), see figure 7. The data compilation shown in figure 7B suggests that $D_{Na}$ may also be similarly controlled, even though Na occupies a interstitial site (Ishikawa & Ichikuni, 1984). This accounts for $D_{Na}$ in *O. ammonoides* 2-3× that of previously studied foraminifera, as test Mg/Ca is two orders of magnitude higher than the species utilised by Wit et al. (2013). Whilst this explains the broad inter-species differences in Na/Ca, it does not negate our discussion of other controls on Na incorporation as a significant complication for this proxy (section 4.3) because the $D_{Na}$-$Mg/Ca_{calcite}$ slope is low; other factors dominantly control Na incorporation within a narrower range of test Mg/Ca ratios.

The nummulitids originated in the late Cretaceous or early Paleocene (Hottinger, 1977) when seawater Mg/Ca was much lower than at present (e.g. Dickson, 2004). Early Cenozoic seawater [Ca] may have been ∼2× present day (Horita et al., 2002) and Mg discrimination during calcification was less important because at this time this biomineralisation mechanism would have produced calcite with an acceptably low Mg/Ca ratio (figure 5) without the requirement for energetically expensive biological processes to modify the chemistry of seawater vacuoles.

The consistency of our data with that of Raitzsch et al. (2010) provides further evidence that this biomineralisation mechanism is common to all nummulitid foraminifera (see also Evans et al. (2013) for data regarding proxy incorporation in *O. complanata* and *Nummulites*). Because Raitzsch et al. (2010) varied seawater

[Ca] and [Mg], whereas we modified only seawater [Mg] in our variable chemistry experiment, these datasets furthermore demonstrate that it is the seawater Mg/Ca ratio that is the dominant control on test chemistry, as also shown by Segev & Erez (2006). This means that the application of these calibrations to fossil foraminifera do not suffer from uncertainty regarding the absolute secular variation in seawater Mg or Ca concentration.

### *4.3. Implications for other proxy systems*

Since Cd/Ca was initially identified as a proxy in foraminiferal calcite (Hester & Boyle, 1982), many other trace element systems have been developed which relate to a number of environmental or physiological parameters (reviewed by Katz et al., 2010). Here, we focus on Li, Na and Ba incorporation because these proxies are actively undergoing refinement and we find multiple controlling factors for each.

Li incorporation into *O. ammonoides* is strongly controlled by both $Li/Ca_{sw}$ and temperature. Whilst we cannot eliminate further complicating factors in the application of foraminifera Li/Ca data based on our cultures, the inconsistent relationship between Li/Ca and $\Omega$ or growth rate between the two experiments strongly suggest that these variables exert at most a relatively minor control on test Li/Ca. The strong correlation observed between seawater and test Li/Ca (figure 6B) has significant implications for the use of Li/Ca or coupled Li-Mg/Ca data for simultaneous $\Delta CO_3^{2-}$-temperature reconstructions (e.g. Bryan & Marchitto, 2008; Lear et al., 2010). Although it is likely that the slope of this relationship (m = 29.0) is steeper than that for planktic or deep benthic foraminifera (cf. Delaney et al., 1985) – our seawater-test Ba/Ca slope is much higher than that of planktic foraminifera – it is clear that relatively small shifts in $Li/Ca_{sw}$ may result in $Li/Ca_{test}$ variation equally as great as that resulting from temperature or $\Delta CO_3^{2-}$. Whilst the relatively

long residence time of Li and Ca in the ocean (2.5-4 Ma and 1-1.5 Ma respectively (Li, 1982)) eliminates secular variation in $Li/Ca_{sw}$ as a complication on glacial-interglacial timescales, such changes may be significant in relation to records spanning several Ma, particularly across geological events such as the early Oligocene glaciation (Lear & Rosenthal, 2006) that might reasonably be expected to be associated with large changes in weathering rates.

Na/Ca in *O. ammonoides* is sensitive to temperature and growth rate across the range that these parameters varied in our experiments, which were at constant salinity within each experiment (variable temperature; variable seawater chemistry). Our data are consistent with that of Delaney et al. (1985), who also found a broad (inter-species) relationship between $Na/Ca_{test}$ and temperature. Our data broadly support those of Wit et al. (2013) in that $Na/Ca_{test}$ is higher in experiments conducted at a salinity of 41‰ compared to those at 37‰, although this may be a result of the higher growth rates in cultures at higher salinity. It is clear that the overprint from growth rate and/or temperature is significant to the point that it is difficult to see how this potential proxy would be applied in the fossil record without some independent constraint of these parameters. Utilising foraminiferal Na/Ca ratios as a palaeosalinity proxy may also be complicated by the location of $Na^+$ ions within the calcite lattice. Because it is likely that a predominant proportion of calcite and aragonite $Na^+$ is located in interstitial sites (Ishikawa & Ichikuni, 1984; Mitsuguchi et al., 2001), this may make fossil Na/Ca especially susceptible to diagenesis.

We find no significant relationship between foraminifera Sr/Ca and any of the investigated variables with the exception of the Mg/Ca ratio of calcite (figure 7), an artefact of the large variation in $Mg/Ca_{test}$ in these experiments which exerts a greater control on $D_{Sr}$ than the other varied parameters (figure 7) and explains the poor correlation between test-seawater Sr/Ca (figure 6N). The much steeper

$D_{Sr}$-$Mg/Ca_{calcite}$ slope of *H. depressa* (Raitzsch et al., 2010) suggests that Mg incorporation is not the only control on $D_{Sr}$ and may be the result of the highly variable saturation state and/or seawater [Ca] and [Mg] of these experiments. However, applying a correction to the data of (Raitzsch et al., 2010) for the variable test Mg/Ca in their experiments suggests that the slope of their $\Omega$-$D_{Sr}$ regression should be reduced from $8.7\times10^{-3}$ to $7.1\times10^{-3}$. Finally, low-Mg planktic and benthic foraminifera such as *Orbulina universa* (Russell et al., 2004) and *Ammonia tepida* (Raitzsch et al., 2010) fall broadly on the same $D_{Sr}$-$Mg/Ca_{calcite}$ line (figure 7), strongly suggesting that the lower Mg/Ca ratio of planktic and low-Mg benthic foraminifera directly results in the lower $D_{Sr}$ of these foraminifera.

Evans et al. (2013) used the inorganic $D_{Sr}$-$Mg/Ca_{calcite}$ relationship to correct Eocene fossil Sr/Ca data before using the calculated $D_{Sr}$ to reconstruct Eocene $Sr/Ca_{sw}$. At the time it was not certain that the data should be corrected in this way but these reconstructions can now be viewed with increased confidence.

The steep test-seawater Ba/Ca slope relative to planktic foraminifera potentially make the nummulitids a more sensitive archive of $Ba/Ca_{sw}$. The shallow depth-distribution of these foraminifera give them the potential to be good indicators of upwelling or freshwater flux to the surface ocean in the fossil record. Whilst there is no growth rate or saturation state control on Ba incorporation based on our data, we observe a significant temperature dependency, although a $\sim$6°C temperature shift is required to produce the same variation in $Ba/Ca_{test}$ as a 1 $\mu$mol mol$^{-1}$ change in $Ba/Ca_{sw}$. Previous studies (e.g. Hönisch et al., 2011) investigating this relationship in planktic foraminifera find no significant temperature dependence on $Ba/Ca_{test}$, implying that it is observable in *O. ammonoides* because unlike planktic foraminifera, the Ba/Ca-temperature sensitivity is greater than analytical uncertainty.

## 5. Conclusion

We have performed laboratory calibrations on the shallow-dwelling large benthic foraminifera species *Operculina ammonoides*, principally in order to investigate the control exerted by temperature and seawater Mg/Ca on Mg incorporation in the calcite test. Based on laser-ablation ICPMS measurements at sub-chamber resolution facilitating unequivocal discrimination of calcite precipitated during culture, we find a Mg/Ca-temperature sensitivity of $\sim$1.7%°C$^{-1}$, in good agreement with the field calibration of Evans et al. (2013), and a $D_{Mg}$-$Mg/Ca_{sw}$ gradient of -1.9$\times10^{-3}$. To our knowledge, this is the first time that this relationship has been investigated in detail in three-dimensional $Mg/Ca_{test}$-$Mg/Ca_{sw}$-temperature space. This coupled calibration provides a way forward in the reconstruction of accurate Mg/Ca-derived palaeotemperatures from time periods with non-modern $Mg/Ca_{sw}$ (pre-Pleistocene), or conversely a method of accurate $Mg/Ca_{sw}$ reconstruction if palaeotemperature can be independently constrained. The similarity between these calibrations and those of inorganic calcite precipitation experiments imply that the biomineralisation mechanism of *O. ammonoides* is fundamentally different to other planktic and benthic species, in that this foraminifera appears to lack a mechanism capable of reducing the Mg/Ca ratio of the calcifying fluid. From a proxy development perspective this may be advantageous as the wealth of information regarding inorganic calcite precipitation is likely to be applicable to the nummulitid foraminifera.

Finally, we show data providing preliminary assessment of other proxy trace element systems (Li, Na, Sr, Ba) in *O. ammonoides*. We find significant multiple controls on Li, Na and Ba incorporation, highlighting the need for a good understanding of the control that all variables exert on such systems, particularly those such as growth rate which are challenging to constrain independently in the fossil

record.

The abundance of fossil *Operculina* and closely related genera in climatically relevant periods of geological time such as the Eocene, and the longevity of these large benthic foraminifera, facilitating palaeo-seasonal proxy retrieval (Evans et al., 2013; Evans & Müller, 2013), make this species, and large benthic species in general, deserving of more detailed investigation.

## Acknowledgements

DE acknowledges a NERC postgraduate studentship at Royal Holloway University of London. The authors acknowledge the Israel Science Foundation for funding the experimental part of this research (ISF grant 551/10 to J.E.). We are grateful to Simon Chenery and Tom Barlow (NERC Isotope Geosciences Laboratory) for performing the seawater analyses and for subsequent discussions of the data. We are indebted to the associate editor Yair Rosenthal and three anonymous reviewers for providing detailed and thoughtful comments which led to significant improvements in the presentation of this work.

## References

Bentov, S., Brownlee, C., & Erez, J. (2009). The role of seawater endocytosis in the biomineralization process in calcareous foraminifera. *Proceedings of the National Academy of Sciences*, *106*, 21500–21504.

Bentov, S., & Erez, J. (2006). Impact of biomineralization processes on the Mg content of foraminiferal shells: A biological perspective. *Geochemistry Geophysics Geosystems*, *7*, Q01P08.

Bryan, S., & Marchitto, T. (2008). Mg/Ca–temperature proxy in benthic foraminifera: New calibrations from the Florida Straits and a hypothesis regarding Mg/Li. *Paleoceanography*, *23*, PA2220.

Burton, E., & Walter, L. (1991). The effects of $pCO_2$ and temperature on magnesium incorporation in calcite in seawater and $MgCl_2$-$CaCl_2$ solutions. *Geochimica et Cosmochimica Acta*, *55*, 777–785.

781 Coggon, R., Teagle, D., Smith-Duque, C., Alt, J., & Cooper, M. (2010). Recon-
782 structing past seawater Mg/Ca and Sr/Ca from mid-ocean ridge flank calcium
783 carbonate veins. *Science*, *327*, 1114–1117.

784 De Choudens-Sánchez, V., & González, L. A. (2009). Calcite and aragonite pre-
785 cipitation under controlled instantaneous supersaturation: Elucidating the role of
786 $CaCO_3$ saturation state and Mg/Ca ratio on calcium carbonate polymorphism.
787 *Journal of Sedimentary Research*, *79*, 363–376.

788 Delaney, M., Bé, A. W. H., & Boyle, E. A. (1985). Li, Sr, Mg, and Na in
789 foraminiferal calcite shells from laboratory culture, sediment traps, and sediment
790 cores. *Geochimica et Cosmochimica Acta*, *49*, 1327–1341.

791 Dickson, J. (2004). Echinoderm skeletal preservation: calcite-aragonite seas and
792 the Mg/Ca ratio of Phanerozoic oceans. *Journal of Sedimentary Research*, *74*,
793 355–365.

794 Erez, J. (2003). The source of ions for biomineralization in foraminifera and their im-
795 plications for paleoceanographic proxies. *Reviews in mineralogy and geochemistry*,
796 *54*, 115–149.

797 Evans, D., & Müller, W. (2012). Deep time foraminifera Mg/Ca paleothermometry:
798 Nonlinear correction for secular change in seawater Mg/Ca. *Paleoceanography*,
799 *PA4205*.

800 Evans, D., & Müller, W. (2013). LA-ICPMS elemental imaging of complex dis-
801 continuous carbonates: An example using large benthic foraminifera. *Journal of*
802 *Analytical Atomic Spectroscopy*, *28*, 1039–1044.

803 Evans, D., Müller, W., Oron, S., & Renema, W. (2013). Eocene seasonality
804 and seawater alkaline earth reconstruction using shallow-dwelling large benthic
805 foraminifera. *Earth and Planetary Science Letters*, *381*, 104–115.

806 Fantle, M., & DePaolo, D. (2006). Sr isotopes and pore fluid chemistry in carbonate
807 sediment of the Ontong Java Plateau: Calcite recrystallization rates and evidence
808 for a rapid rise in seawater Mg over the last 10 million years. *Geochimica et*
809 *Cosmochimica Acta*, *70*, 3883–3904.

810 Guido, A., Papazzoni, C., Mastandrea, A., Morsilli, M., La Russa, M., Tosti, F., &
811 Russo, F. (2011). Automicrite in a 'nummulite bank' from the Monte Saraceno
812 (Southern Italy): evidence for synsedimentary cementation. *Sedimentology*, *58*,
813 878–889.

814 Hasiuk, F., & Lohmann, K. (2010). Application of calcite Mg partitioning functions
815 to the reconstruction of paleocean Mg/Ca. *Geochimica et Cosmochimica Acta*, *74*,
816 6751–6763.

817 Haywood, A., Ridgwell, A., Lunt, D., Hill, D., Pound, M., Dowsett, H., Dolan, A.,
818 Francis, J., Williams, M., Haywood, A. et al. (2011). Are there pre-quaternary
819 geological analogues for a future greenhouse warming? *Philosophical Transactions*
820 *of the Royal Society A: Mathematical, Physical and Engineering Sciences*, *369*,
821 933–956.

822 Hester, K., & Boyle, E. (1982). Water chemistry control of cadmium content in
823 recent benthic foraminifera. *Nature*, *298*, 260–262.

824 Hönisch, B., Allen, K., Russell, A., Eggins, S., Bijma, J., Spero, H., Lea, D., &
825 Yu, J. (2011). Planktic foraminifers as recorders of seawater Ba/Ca. *Marine*
826 *Micropaleontology*, *79*, 52–57.

827 Horita, J., Zimmermann, H., & Holland, H. (2002). Chemical evolution of seawa-
828 ter during the Phanerozoic: Implications from the record of marine evaporites.
829 *Geochimica et Cosmochimica Acta*, *66*, 3733–3756.

830 Hottinger, L. (1977). *Foraminifères Operculiniformes* volume 40 of *Série C, Sciences*
831 *de la Terre*. Mémoires du Muséum National d'Histoire Naturelle.

832 Ishikawa, M., & Ichikuni, M. (1984). Uptake of sodium and potassium by calcite.
833 *Chemical geology*, *42*, 137–146.

834 Jochum, K., Stoll, B., Herwig, K., Willbold, M., Hofmann, A., Amini, M., Aarburg,
835 S., Abouchami, W., Hellebrand, E., Mocek, B. et al. (2006). MPI-DING reference
836 glasses for in situ microanalysis: New reference values for element concentrations
837 and isotope ratios. *Geochemistry Geophysics Geosystems*, *7*.

838 Katz, M., Cramer, B., Franzese, A., Hönisch, B., Miller, K., Rosenthal, Y., & Wright,
839 J. (2010). Traditional and emerging geochemical proxies in foraminifera. *The*
840 *Journal of Foraminiferal Research*, *40*, 165–192.

841 Kisakürek, B., Eisenhauer, A., Bohm, F., Garbe-Schönberg, D., & Erez, J. (2008).
842 Controls on shell Mg/Ca and Sr/Ca in cultured planktonic foraminiferan, *Glo-*
843 *bigerinoides ruber* (white). *Earth and Planetary Science Letters*, *273*, 260–269.

844 ter Kuile, B., & Erez, J. (1987). Uptake of inorganic carbon and internal carbon
845 cycling in symbiont-bearing benthonic foraminifera. *Marine Biology*, *94*, 499–509.

ter Kuile, B., Erez, J., & Padan, E. (1989). Mechanisms for the uptake of inorganic carbon by two species of symbiont-bearing foraminifera. *Marine Biology*, *103*, 241–251.

Lea, D. W., & Spero, H. J. (1992). Experimental determination of barium uptake in shells of the planktonic foraminifera *Orbulina universa* at 22°C. *Geochimica et Cosmochimica Acta*, *56*, 2673–2680.

Lear, C., Mawbey, E., & Rosenthal, Y. (2010). Cenozoic benthic foraminiferal Mg/Ca and Li/Ca records: Toward unlocking temperatures and saturation states. *Paleoceanography*, *25*, PA4215.

Lear, C. H., Elderfield, H., & Wilson, P. A. (2000). Cenozoic deep-sea temperatures and global ice volumes from Mg/Ca in benthic foraminiferal calcite. *Science*, *287*, 269–272.

Lear, C. H., & Rosenthal, Y. (2006). Benthic foraminiferal Li/Ca: Insights into Cenozoic seawater carbonate saturation state. *Geology*, *34*, 985–988.

Lear, C. H., Rosenthal, Y., & Slowey, N. (2002). Benthic foraminiferal Mg/Ca-paleothermometry: A revised core-top calibration. *Geochimica et Cosmochimica Acta*, *66*, 3375–3387.

Lebel, J., & Poisson, A. (1976). Potentiometric determination of calcium and magnesium in seawater. *Marine Chemistry*, *4*, 321–332.

Lewis, E., & Wallace, D. (2006). Program developed for $CO_2$ system calculations. *ORNL/CDIAC-105. Carbon Dioxide Information Analysis Center, Oak Ridge National Laboratory, US Department of Energy, Oak Ridge, Tennessee*, .

Li, Y.-H. (1982). A brief discussion on the mean oceanic residence time of elements. *Geochimica et Cosmochimica Acta*, *46*, 2671–2675.

Millero, F. J. (1996). *Chemical Oceanography*. (2nd ed.). Florida: CRC Press.

Mitsuguchi, T., Uchida, T., Matsumoto, E., Isdale, P. J., & Kawana, T. (2001). Variations in Mg/Ca, Na/Ca, and Sr/Ca ratios of coral skeletons with chemical treatments: Implications for carbonate geochemistry. *Geochimica et Cosmochimica Acta*, *65*, 2865–2874.

Mucci, A., & Morse, J. (1983). The incorporation of $Mg^{2+}$ and $Sr^{2+}$ into calcite overgrowths: influences of growth rate and solution composition. *Geochimica et Cosmochimica Acta*, *47*, 217–233.

878 Müller, W., Shelley, M., Miller, P., & Broude, S. (2009). Initial performance metrics
879 of a new custom–designed ArF excimer LA–ICPMS system coupled to a two-
880 volume laser–ablation cell. *Journal of Analytical Atomic Spectrometry*, *24*, 209–
881 214.

882 de Nooijer, L. J., Toyofuku, T., & Kitazato, H. (2009). Foraminifera promote calci-
883 fication by elevating their intracellular pH. *Proceedings of the National Academy*
884 *of Sciences*, *106*, 15374–15378.

885 Nürnberg, D., Bijma, J., & Hemleben, C. (1996). Assessing the reliability of magne-
886 sium in foraminiferal calcite as a proxy for water mass temperatures. *Geochimica*
887 *et Cosmochimica Acta*, *60*, 803–814.

888 Okumura, M., & Kitano, Y. (1986). Coprecipitation of alkali metal ions with calcium
889 carbonate. *Geochimica et Cosmochimica Acta*, *50*, 49–58.

890 Oomori, T., Kaneshima, H., Maezato, Y., & Kitano, Y. (1987). Distribution coeffi-
891 cient of $Mg^{2+}$ ions between calcite and solution at 10–50°C. *Marine Chemistry*,
892 *20*, 327–336.

893 Raitzsch, M., Dueñas-Bohórquez, A., Reichart, G.-J., de Nooijer, L., & Bickert, T.
894 (2010). Incorporation of Mg and Sr in calcite of cultured benthic foraminifera:
895 impact of calcium concentration and associated calcite saturation state. *Biogeo-*
896 *sciences*, *7*, 869–881.

897 Reiss, Z. (1958). Classification of lamellar foraminifera. *Micropaleontology*, *4*, 51–70.

898 Ries, J. (2004). Effect of ambient Mg/Ca ratio on Mg fractionation in calcareous
899 marine invertebrates: A record of the oceanic Mg/Ca ratio over the Phanerozoic.
900 *Geology*, *32*, 981–984.

901 Rosenthal, Y., Boyle, E. A., & Slowey, N. (1997). Temperature control on the
902 incorporation of magnesium, strontium, fluorine, and cadmium into benthic
903 foraminiferal shells from Little Bahama Bank: Prospects for thermocline pale-
904 oceanography. *Geochimica et Cosmochimica Acta*, *61*, 3633–3643.

905 Russell, A., Hönisch, B., Spero, H., & Lea, D. (2004). Effects of seawater carbonate
906 ion concentration and temperature on shell U, Mg, and Sr in cultured planktonic
907 foraminifera. *Geochimica et cosmochimica acta*, *68*, 4347–4361.

908 Segev, E., & Erez, J. (2006). Effect of Mg/Ca ratio in seawater on shell composition
909 in shallow benthic foraminifera. *Geochemistry, Geophysics, Geosystems*, *7*.

910 Stanley, S., & Hardie, L. (1998). Secular oscillations in the carbonate mineralogy
911 of reef-building and sediment-producing organisms driven by tectonically forced
912 shifts in seawater chemistry. *Palaeogeography, Palaeoclimatology, Palaeoecology*,
913 *144*, 3–19.

914 Pogge von Strandmann, P. A. (2008). Precise magnesium isotope measurements in
915 core top planktic and benthic foraminifera. *Geochemistry, Geophysics, Geosys-*
916 *tems*, *9*.

917 Toyofuku, T., Kitazato, H., Kawahata, H., Tsuchiya, M., & Nohara, M. (2000).
918 Evaluation of Mg/Ca thermometry in foraminifera: Comparison of experimental
919 results and measurements in nature. *Paleoceanography*, *15*, 456–464.

920 de Villiers, S. (1999). Seawater strontium and Sr/Ca variability in the Atlantic and
921 Pacific oceans. *Earth and Planetary Science Letters*, *171*, 623–634.

922 Wit, J., Nooijer, L. d., Wolthers, M., & Reichart, G. (2013). A novel salinity proxy
923 based on Na incorporation into foraminiferal calcite. *Biogeosciences*, *10*, 6375–
924 6387.

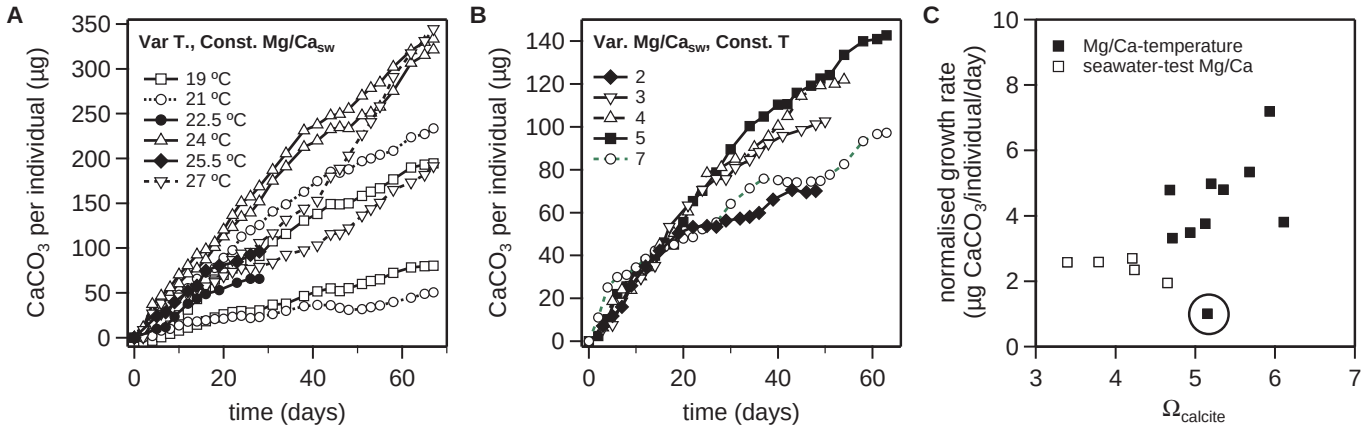


Figure 1: Cumulative growth rates for each culture within (A) the variable temperature, constant seawater chemistry experiment (DE1) and (B) the variable seawater chemistry, constant temperature experiment (DE2). (C) The relationship between growth rate and mean calcite saturation state. With the exception of culture DE1-4 (highlighted), normalised growth rate is broadly positively correlated with $\Omega_{\mathrm{calcite}}$ (see text for details).

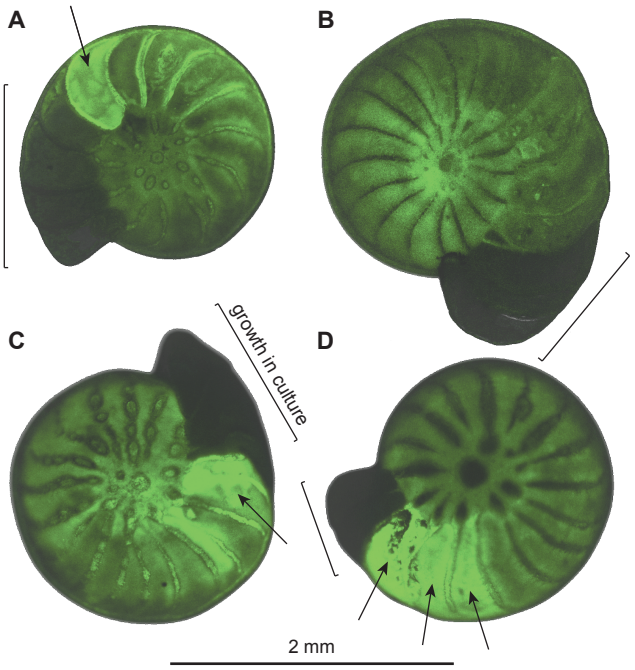


Figure 2: Fluorescent confocal microscope images of calcein labelled *O. ammonoides*. Chambers that were grown during the calcein labelling period (48 hours) are highlighted with arrows, marking the point from which calcite was first grown under controlled culture conditions (see text for details). Note that the specimen shown in B did not form any chambers during the labelling period but formed three chambers subsequently, brackets show chambers precipitated during the experimental period. In addition, all four specimens added secondary laminae to the existing chambers, which is the reason that the majority of the foraminifera are weakly fluorescent.

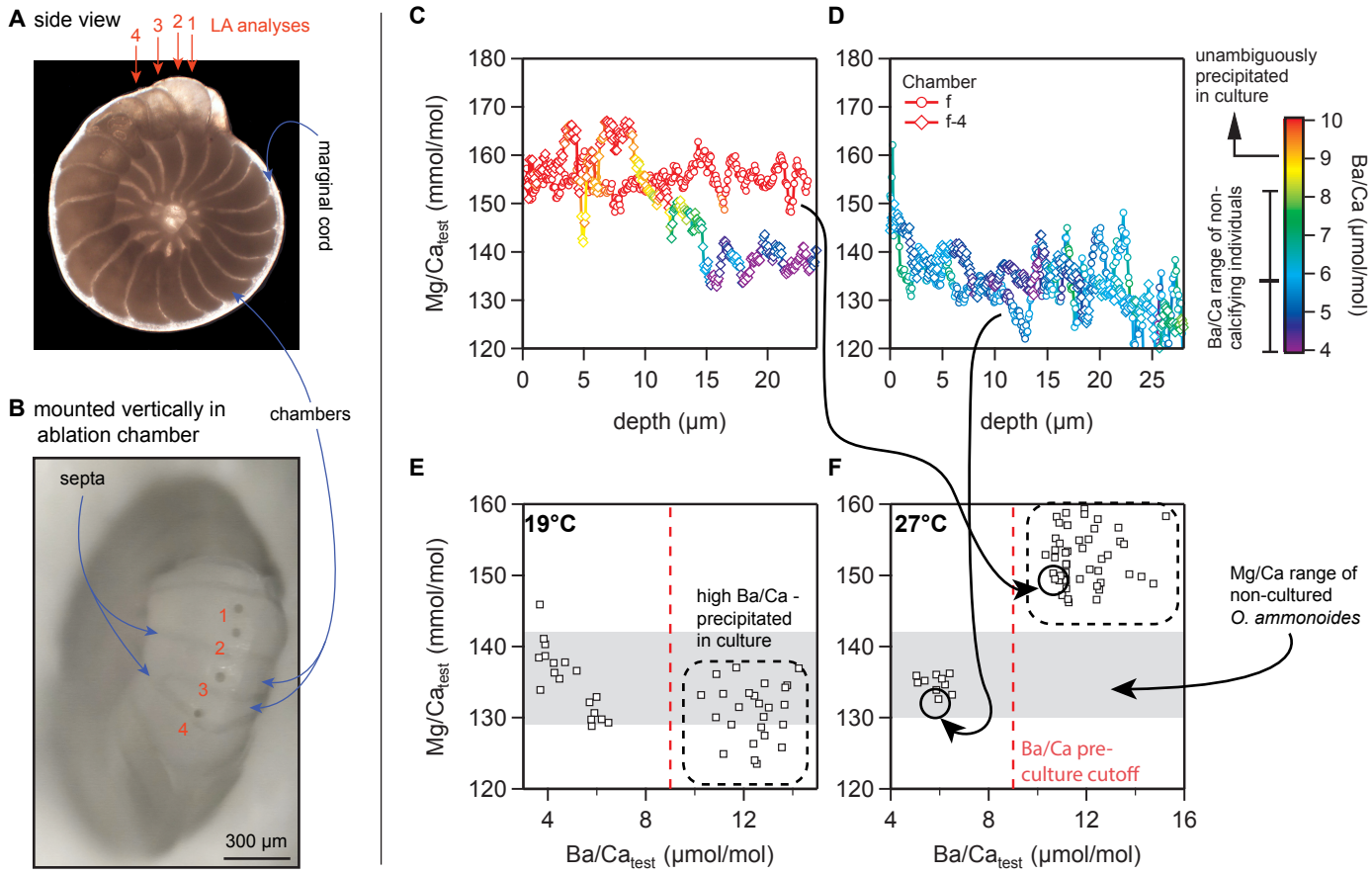


Figure 3: (A) Live *Operculina ammonoides* under cross-polarised light. (B) Post-analysis view of a specimen mounted sub-vertically in the ablation chamber. Laser craters are 44 $\mu$m in diameter. (C-F) Using a seawater Ba-spike (0.15 $\mu$M) in order to identify material precipitated during the culture period. (C) A specimen cultured at 27°C that precipitated new chambers during the culture period (elevated test Ba/Ca) and (D) a specimen that stopped calcifying when placed in culture. Ba/Ca ratios are shown as a function of colour. 11-point Mg/Ca running means are plotted. Time was converted to depth assuming that each laser pulse removes 80 nm of calcite. (E,F) All analyses for the 19°C and the 27°C Mg/Ca-temperature calibration experiments respectively, demonstrating the effectiveness of this technique at discriminating newly formed and pre-existing calcite. Mg/Ca is relatively lower and higher in experiments conducted at 19°C and 27°C respectively compared to pre-culture calcite, as expected given that these foraminifera were taken from seawater with a winter-spring average temperature of ~22°C.

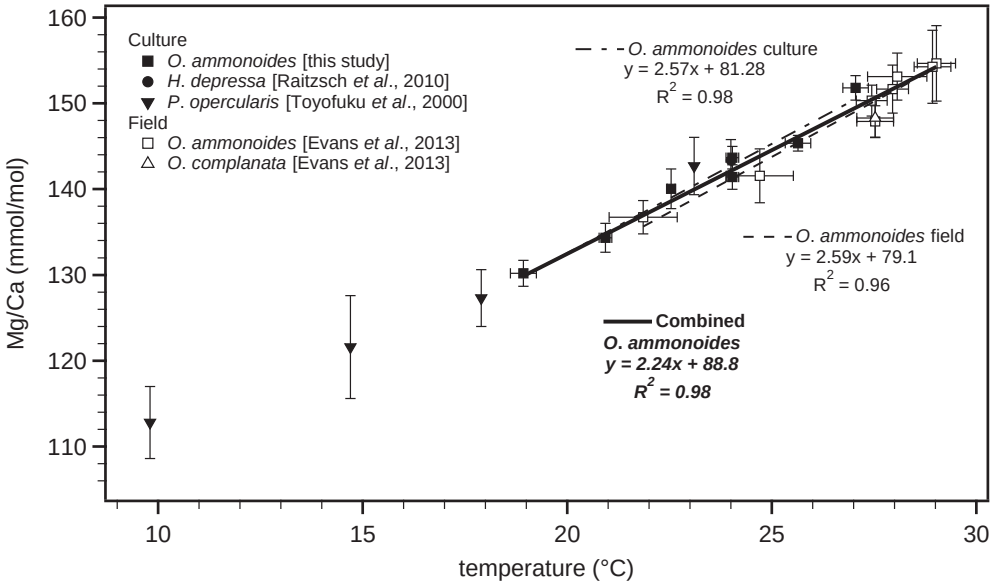


Figure 4: The relationship between $Mg/Ca_{test}$ and temperature in laboratory cultured *Operculina ammonoides* in the context of a comparative field-based calibration (Evans et al., 2013), data from other species within the family Nummulitidae and *P. opercularis* (Toyofuku et al., 2000), an unrelated shallow benthic foraminifera with a Mg/Ca-temperature sensitivity within error of that for *Operculina*. The datapoint of Raitzsch et al. (2010) is not visible as it lies almost precisely below the data presented here (24°C, Mg/Ca = 143.3 mmol $mol^{-1}$). A regression through the *P. opercularis* data is within error of that for the nummulitids (m = 2.23, c = 89.6). We recommend using the 'combined' calibration for palaeoceanic reconstruction. Mg/Ca error bars are 2SE, temperature error bars are 2SD.

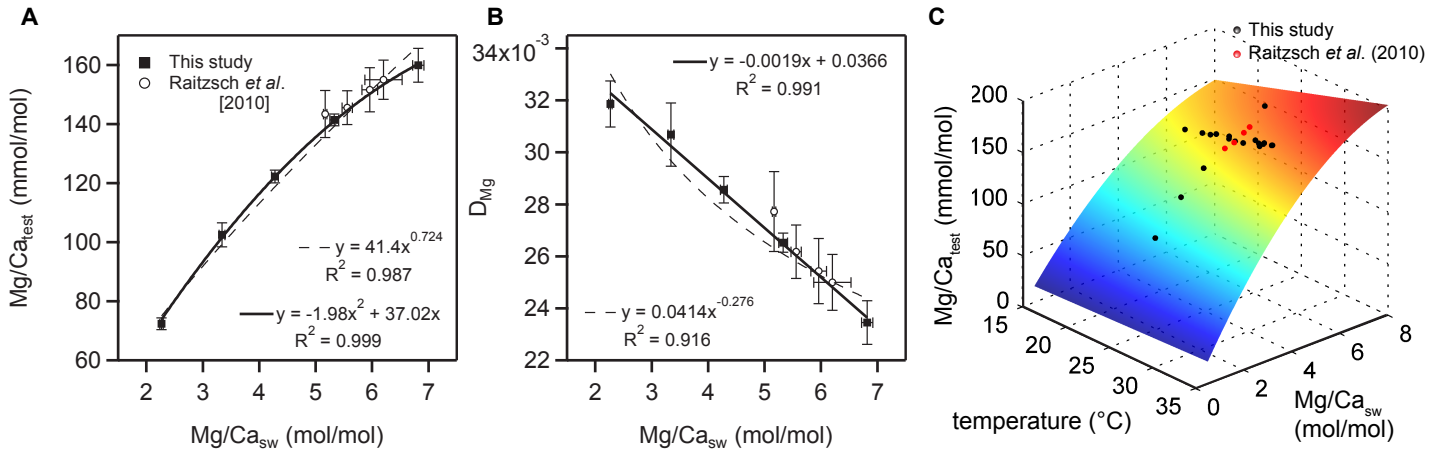


Figure 5: The relationship between (A) test Mg/Ca and (B) the Mg/Ca distribution coefficient with seawater Mg/Ca. The linear relationship between $D_{Mg}$ and $Mg/Ca_{sw}$ implies a 2$^{nd}$ order polynomial relationship between $Mg/Ca_{sw}$-$Mg/Ca_{test}$, passing through the origin. Power-law regressions are shown for comparison. Error bars are ±2SE. (C) A coupled $Mg/Ca_{test}$-$Mg/Ca_{sw}$-temperature calibration showing the surface defined by equation 10 as well as the laboratory culture data of this study and Raitzsch et al. (2010). Colour is shown as a function of $Mg/Ca_{test}$ (z-axis height). Regressions derived from *O. ammonoides* data only.

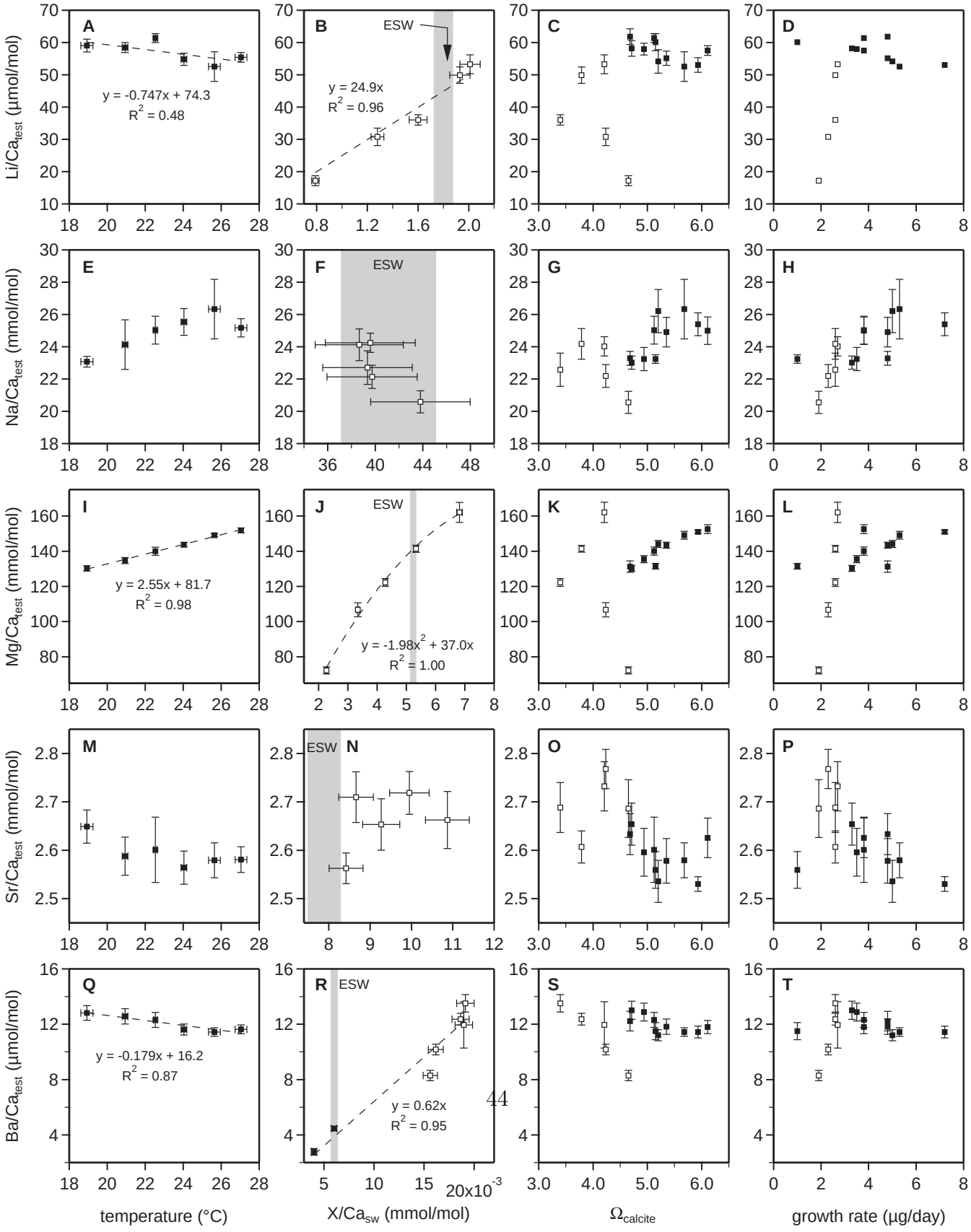




Figure 6: Caption on following page.

Figure 6: Li-Na-Mg-Sr-Ba relationships with temperature, seawater chemistry, mean saturation state and growth rate. A normalisation factor was applied to the growth rate in order to correct for potential bias relating to foraminifera which did not calcify at all; growth rate is calculated from alkalinity, individual foraminifera were not monitored which may be a cause of significant inaccuracy in these estimates. Closed symbols represent data from the variable temperature experiment and open symbols represent data from the variable seawater chemistry experiment. Repeat experiments under equivalent conditions were not pooled for these plots because growth rate and calculated carbonate chemistry varied between these repeats. Error bars are 2SE for LA-ICPMS foraminifera data and 2SD precision for seawater data.

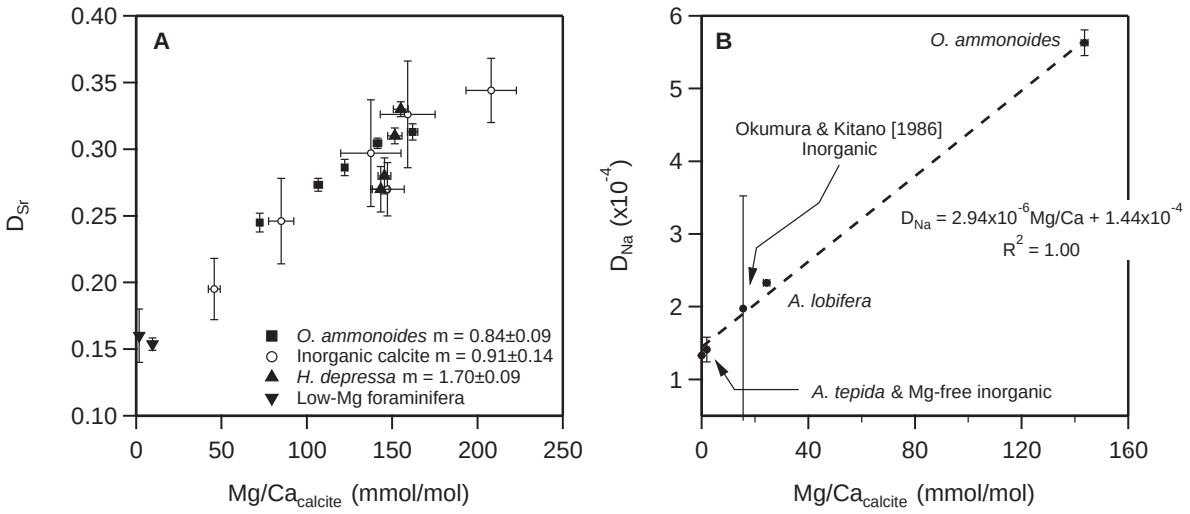


Figure 7: (A) The relationship between $Mg/Ca_{calcite}$ and $D_{Sr}$. Our data for *O. ammonoides* fall on the same trend as that for inorganic calcite (Mucci & Morse, 1983). The analyses of Raitzsch et al. (2010) of the closely related foraminifera *H. depressa* are also broadly consistent with this trend, as are data from low-Mg planktic (*O. universa*; Russell et al., 2004) and benthic (*A. tepida*; Raitzsch et al., 2010) foraminifera. (B) $D_{Na}$ variation is similarly related to $Mg/Ca_{calcite}$ when a wide range of calcites are considered, implying that lattice distortion from Mg incorporation may also allow more alkali metal ions into interstitial sites.

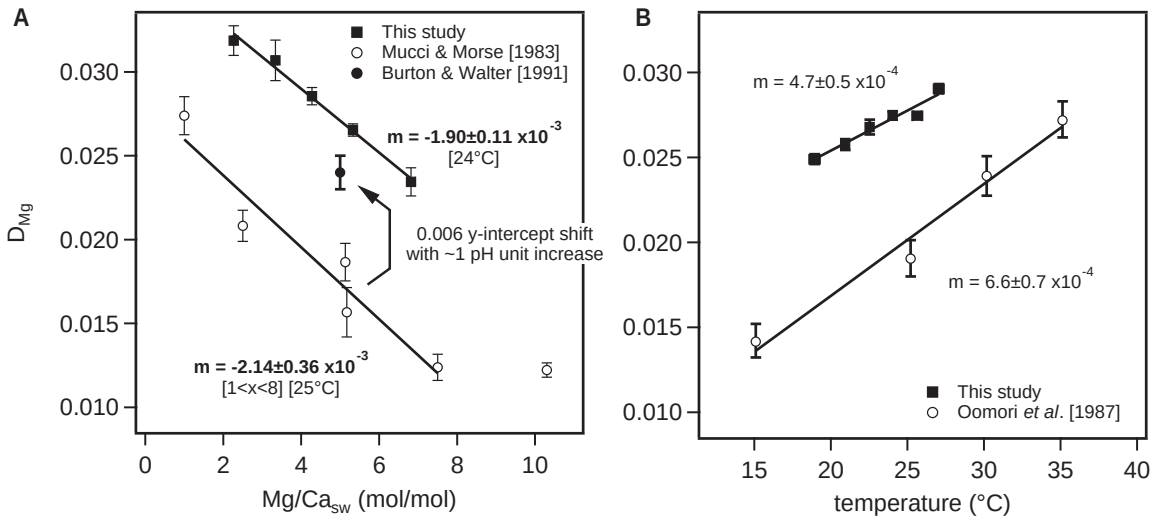


Figure 8: A comparison of the relationship between (A) $D_{Mg}$ and $Mg/Ca_{sw}$ and (B) $D_{Mg}$ and temperature in *O. ammonoides* and inorganic calcite (Mucci & Morse, 1983; Oomori et al., 1987). The $D_{Mg}$-$Mg/Ca_{sw}$ slopes are within error of each other. The pH-$D_{Mg}$ calibrations of Burton & Walter (1991) may provide an explanation for the offset in y-intercept of these foraminifera compared to inorganic calcite, as inorganic precipitation experiments at elevated pH are offset to higher $D_{Mg}$ values, and foraminifera are known to elevate the pH of internal seawater vacuoles.

Table 1: Summary of experimental temperature and seawater characteristics for all foraminifera cultures. ESW and ASW denote natural Gulf of Eilat seawater and artificial seawater prepared with no Mg respectively. The increased alkalinity uncertainty for groups DE2-17(6) and 16(5) is the result of the preparation of new reservoirs with higher alkalinity midway through the experiment.

| Sample prefix | Temp. (°C) | $Mg/Ca_{sw}$ (mol $mol^{-1}$) | [Ca] (mM) | Ratio ESW:ASW | Salinity (‰) | pH | Alkalinity (mEq $l^{-1}$) |
|---|---|---|---|---|---|---|---|
| | | Experiment 1: Variable temperature | | | | | |
| (DE1-) 1-8; 24; 25 | 19-27 | 5.42 | 12.3 | 1:0 | 40.7 | 8.05 | 2.487-2.503 |
| | | Experiment 2: Variable $Mg/Ca_{sw}$ | | | | | |
| DE2-17(6) | 24 | 6.82 | 10.7 | 1:0 | 38.0 | 8.09 | 2.175±0.143 |
| DE2-16(5) | 24 | 5.33 | 10.6 | 1:0 | 37.0 | 8.05 | 2.243±0.086 |
| DE2-20(7) | 24 | 4.28 | 11.3 | 4:1 | 37.0 | 7.98 | 2.318±0.018 |
| DE2-21(8) | 24 | 3.34 | 11.7 | 3:2 | 37.0 | 8.04 | 2.505±0.021 |
| DE2-22(9) | 24 | 2.27 | 11.4 | 2:3 | 37.0 | 8.14 | 2.502±0.022 |

Table 2: Reservoir and cumulative water sample carbonate chemistry and indicators of growth rate. Column $n_1$ gives the number of foraminifera that added at least one new chamber (the number of foraminifera analysed is shown in brackets) based on specimens with at least one analysis characterised by elevated Ba/Ca. Column $n_2$ gives the number of laser ablation depth-profiles positioned on calcite precipitated during the experimental period (the total number of analyses are shown in brackets). Normalised growth rate = growth rate × (total foraminifera analysed)/(foraminifera that precipitated at least one chamber in culture).

| | | reservoir | | cumulative samples | | | | | | growth rate | |
|---|---|---|---|---|---|---|---|---|---|---|---|
| Culture | Temp. (°C) | Ω | $[CO_3^{2-}]$ ($\mu$M) | alkalinity ($\mu$Eq $l^{-1}$) | pH | Ω | $[CO_3^{2-}]$ ($\mu$M) | $n_1$ | $n_2$ | mean ($\mu$g $CaCO_3$ $ind.^{-1}$ $d^{-1}$) | normalised |
| DE1-1 | 18.9 | 5.11 | 224 | 2443 | 7.99 | 4.31 | 189 | 7(8) | 23(37) | 2.9 | 3.3 |
| DE1-2 | 18.9 | 5.11 | 224 | 2474 | 7.97 | 4.25 | 187 | 2(8) | 8(42) | 1.2 | 4.8 |
| DE1-3 | 20.9 | 5.42 | 238 | 2432 | 7.98 | 4.45 | 195 | 8(8) | 27(35) | 3.5 | 3.5 |
| DE1-4 | 20.9 | 5.42 | 238 | 2482 | 8.01 | 4.88 | 214 | 3(4) | 8(19) | 0.8 | 1.0 |
| DE1-24 | 22.5 | 5.67 | 249 | 2460 | 7.96 | 4.58 | 201 | 5(8) | 14(37) | 2.3 | 3.8 |
| DE1-5 | 24.0 | 5.93 | 260 | 2411 | 7.97 | 4.77 | 209 | 8(8) | 30(37) | 4.8 | 4.8 |
| DE1-6 | 24.0 | 5.93 | 260 | 2404 | 7.94 | 4.47 | 196 | 4(4) | 14(16) | 5.0 | 5.0 |
| DE1-25 | 25.6 | 6.20 | 272 | 2436 | 7.98 | 5.16 | 226 | 9(14) | 25(73) | 3.4 | 5.3 |
| DE1-7 | 27.0 | 6.48 | 284 | 2404 | 7.98 | 5.39 | 236 | 5(7) | 23(36) | 5.1 | 7.2 |
| DE1-8 | 27.0 | 6.48 | 284 | 2443 | 8.02 | 5.74 | 251 | 6(8) | 26(51) | 2.9 | 3.8 |
| DE2-17(6) | 24.0 | 5.31 | 227 | 2067 | 7.84 | 3.10 | 132 | 4(7) | 9(30) | 1.5 | 2.7 |
| DE2-16(5) | 24.0 | 5.09 | 215 | 2317 | 7.67 | 2.49 | 105 | 7(8) | 27(36) | 2.3 | 2.6 |
| DE2-20(7) | 24.0 | 4.65 | 197 | 2517 | 7.56 | 2.14 | 91 | 7(8) | 27(35) | 2.3 | 2.6 |
| DE2-21(8) | 24.0 | 5.61 | 237 | 2451 | 7.71 | 2.86 | 121 | 7(8) | 26(32) | 2.1 | 2.3 |
| DE2-22(9) | 24.0 | 6.66 | 282 | 2456 | 7.67 | 2.64 | 112 | 6(8) | 20(34) | 1.5 | 1.9 |

Table 3: Seawater and foraminifera trace element data measured by solution and laser-ablation ICPMS respectively. Seawater analyses shown are of the reservoir water samples. Laser ablation data represent the mean of all analyses of newly precipitated calcite. Errors are precision (±2SD) for seawater analyses as the number of analyses was relatively small (n = <10), and ±2SE for laser-ablation data where n was typically greater than 30 (see table 2).

| Culture | | | value | | | | | error | | |
|---|---|---|---|---|---|---|---|---|---|---|
| **Seawater** | Li/Ca mmol mol$^{-1}$ | Na/Ca mol mol$^{-1}$ | Mg/Ca mol mol$^{-1}$ | Sr/Ca mmol mol$^{-1}$ | Ba/Ca $\mu$mol mol$^{-1}$ | Li/Ca mmol mol$^{-1}$ | Na/Ca mol mol$^{-1}$ | Mg/Ca mol mol$^{-1}$ | Sr/Ca mmol mol$^{-1}$ | Ba/Ca $\mu$mol mol$^{-1}$ |
| | | | (1) – Gulf of Eilat at the time of collection | | | | | | | |
| | 1.80 | 41.1 | 5.23 | 7.89 | 6.01 | 0.07 | 3.9 | 0.08 | 0.38 | 0.28 |
| | | | (2) – Experiment reservoirs | | | | | | | |
| DE1-$x$ | 2.10 | 45.3 | 5.23 | 8.59 | 17.59 | 0.09 | 4.3 | 0.08 | 0.42 | 0.81 |
| DE2-17(6) | 2.01 | 42.6 | 6.82 | 8.66 | 18.98 | 0.08 | 4.1 | 0.10 | 0.42 | 0.87 |
| DE2-16(5) | 1.93 | 41.6 | 5.33 | 8.42 | 18.65 | 0.08 | 4.0 | 0.08 | 0.41 | 0.86 |
| DE2-20(7) | 1.60 | 42.3 | 4.28 | 9.27 | 19.13 | 0.07 | 4.0 | 0.06 | 0.45 | 0.88 |
| DE2-21(8) | 1.28 | 42.7 | 3.34 | 9.95 | 16.18 | 0.05 | 4.1 | 0.05 | 0.48 | 0.74 |
| DE2-22(9) | 0.79 | 47.1 | 2.27 | 10.87 | 15.63 | 0.03 | 4.5 | 0.03 | 0.53 | 0.72 |
| **Foraminifera** | Li/Ca $\mu$mol mol$^{-1}$ | Na/Ca mmol mol$^{-1}$ | Mg/Ca mmol mol$^{-1}$ | Sr/Ca mmol mol$^{-1}$ | Ba/Ca $\mu$mol mol$^{-1}$ | Li/Ca $\mu$mol mol$^{-1}$ | Na/Ca mmol mol$^{-1}$ | Mg/Ca mmol mol$^{-1}$ | Sr/Ca mmol mol$^{-1}$ | Ba/Ca $\mu$mol mol$^{-1}$ |
| | | | (1) – Non-calcifying individuals | | | | | | | |
| | 55.7 | 25.1 | 137.3 | 2.61 | 4.6 | 1.1 | 0.5 | 1.0 | 0.03 | 0.2 |
| | | | (2) – Individual cultures | | | | | | | |
| DE1-1 | 58.2 | 23.0 | 129.9 | 2.65 | 13.0 | 2.4 | 0.4 | 1.6 | 0.04 | 0.7 |
| DE1-2 | 61.8 | 23.3 | 131.2 | 2.63 | 12.2 | 2.4 | 0.4 | 1.6 | 0.04 | 0.7 |
| DE1-3 | 58.0 | 23.2 | 135.5 | 2.60 | 12.9 | 1.8 | 0.7 | 2.0 | 0.05 | 0.6 |
| DE1-4 | 60.1 | 23.2 | 131.4 | 2.56 | 11.5 | 2.6 | 0.3 | 1.7 | 0.04 | 0.6 |
| DE1-24 | 61.4 | 25.0 | 140.0 | 2.60 | 12.3 | 1.4 | 0.9 | 2.4 | 0.07 | 0.5 |
| DE1-5 | 55.1 | 24.9 | 143.4 | 2.58 | 11.8 | 2.2 | 0.9 | 1.7 | 0.05 | 0.6 |
| DE1-6 | 54.1 | 26.2 | 144.2 | 2.54 | 11.2 | 3.6 | 1.3 | 2.0 | 0.04 | 0.4 |
| DE1-25 | 55.6 | 26.3 | 149.1 | 2.58 | 11.4 | 4.6 | 1.8 | 2.2 | 0.04 | 0.3 |
| DE1-7 | 53.0 | 25.4 | 151.0 | 2.53 | 11.4 | 2.3 | 0.7 | 1.0 | 0.02 | 0.4 |
| DE1-8 | 57.5 | 25.0 | 152.5 | 2.63 | 11.8 | 1.5 | 0.8 | 2.5 | 0.04 | 0.5 |
| DE2-17(6) | 53.3 | 24.2 | 162.0 | 2.71 | 12.0 | 2.9 | 0.6 | 5.7 | 0.05 | 1.7 |
| DE2-16(5) | 49.9 | 24.1 | 141.4 | 2.56 | 12.4 | 2.6 | 1.0 | 2.0 | 0.03 | 0.4 |
| DE2-20(7) | 36.0 | 22.7 | 122.2 | 2.65 | 13.5 | 1.6 | 1.0 | 2.2 | 0.05 | 0.6 |
| DE2-21(8) | 30.7 | 22.1 | 106.7 | 2.72 | 10.2 | 2.7 | 0.7 | 4.0 | 0.04 | 0.4 |
| DE2-22(9) | 17.2 | 20.6 | 72.3 | 2.66 | 8.3 | 1.6 | 0.7 | 2.0 | 0.06 | 0.4 |
| | | | (3) – Pooled duplicates | | | | | | | |
| 19.0°C | 59.1 | 23.1 | 130.2 | 2.65 | 12.8 | 2.0 | 0.3 | 0.7 | 0.03 | 0.5 |
| 21.0°C | 58.5 | 24.1 | 134.6 | 2.59 | 12.6 | 1.6 | 1.5 | 1.7 | 0.04 | 0.6 |
| 22.5°C | 61.4 | 25.0 | 140.0 | 2.60 | 12.3 | 1.4 | 0.9 | 2.4 | 0.07 | 0.5 |
| 24.0°C | 54.8 | 25.5 | 143.6 | 2.56 | 11.6 | 1.9 | 0.8 | 1.3 | 0.03 | 0.4 |
| 25.5°C | 55.6 | 26.3 | 149.1 | 2.58 | 11.4 | 4.6 | 1.8 | 2.2 | 0.04 | 0.3 |
| 27.0°C | 55.4 | 25.2 | 151.8 | 2.58 | 11.6 | 1.5 | 0.6 | 1.4 | 0.03 | 0.3 |

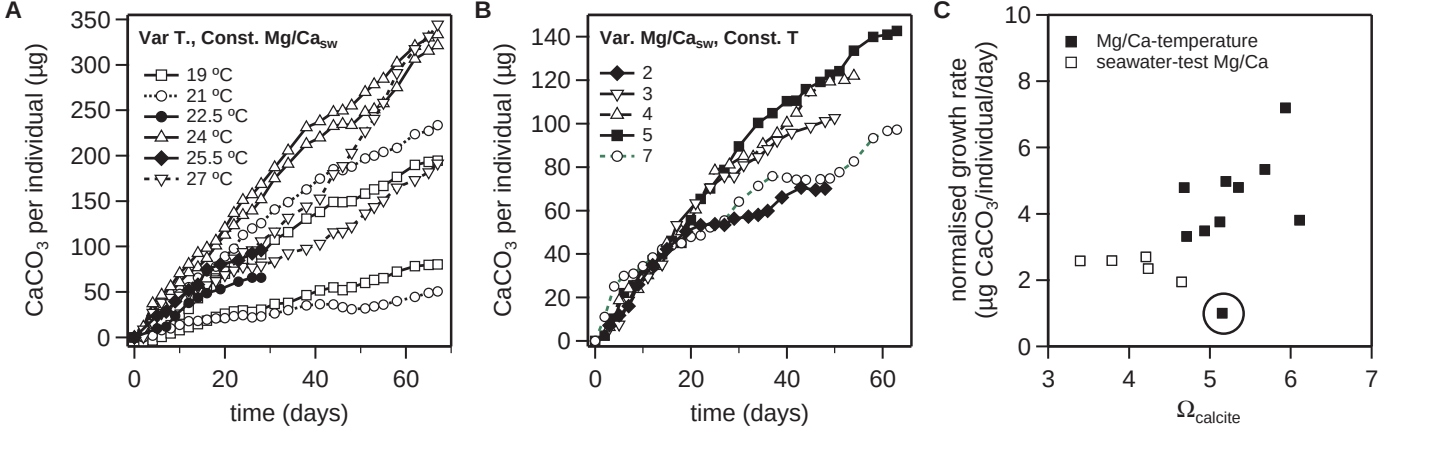
A
Var T., Const. Mg/Ca$_{sw}$
19 ºC
21 ºC
22.5 ºC
24 ºC
25.5 ºC
27 ºC
CaCO$_3$ per individual (µg)
time (days)
B
Var. Mg/Ca$_{sw}$, Const. T
2
3
4
5
7
CaCO$_3$ per individual (µg)
time (days)
C
Mg/Ca-temperature
seawater-test Mg/Ca
normalised growth rate
(µg CaCO$_3$/individual/day)
$\Omega_{calcite}$

Figure2

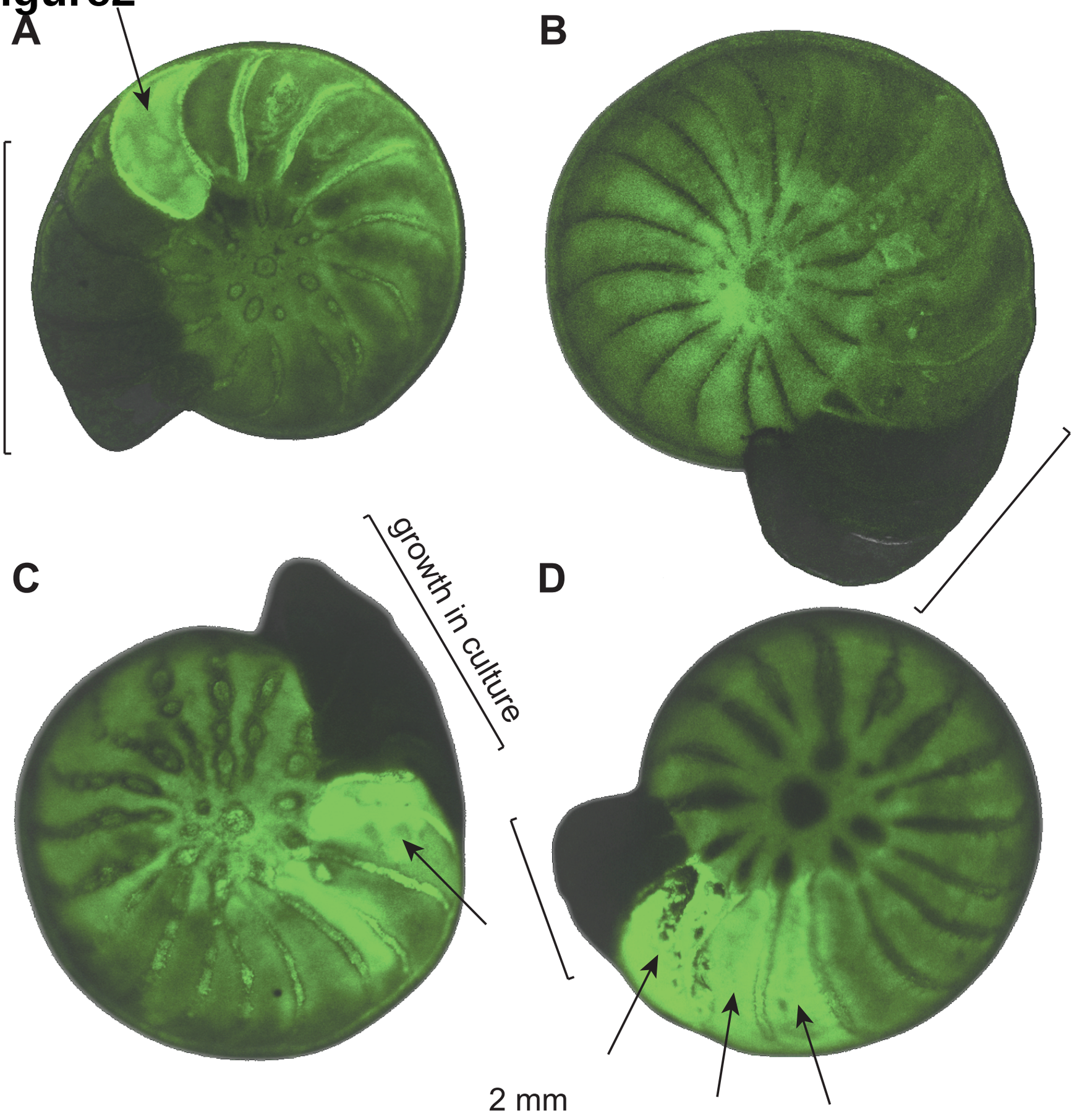

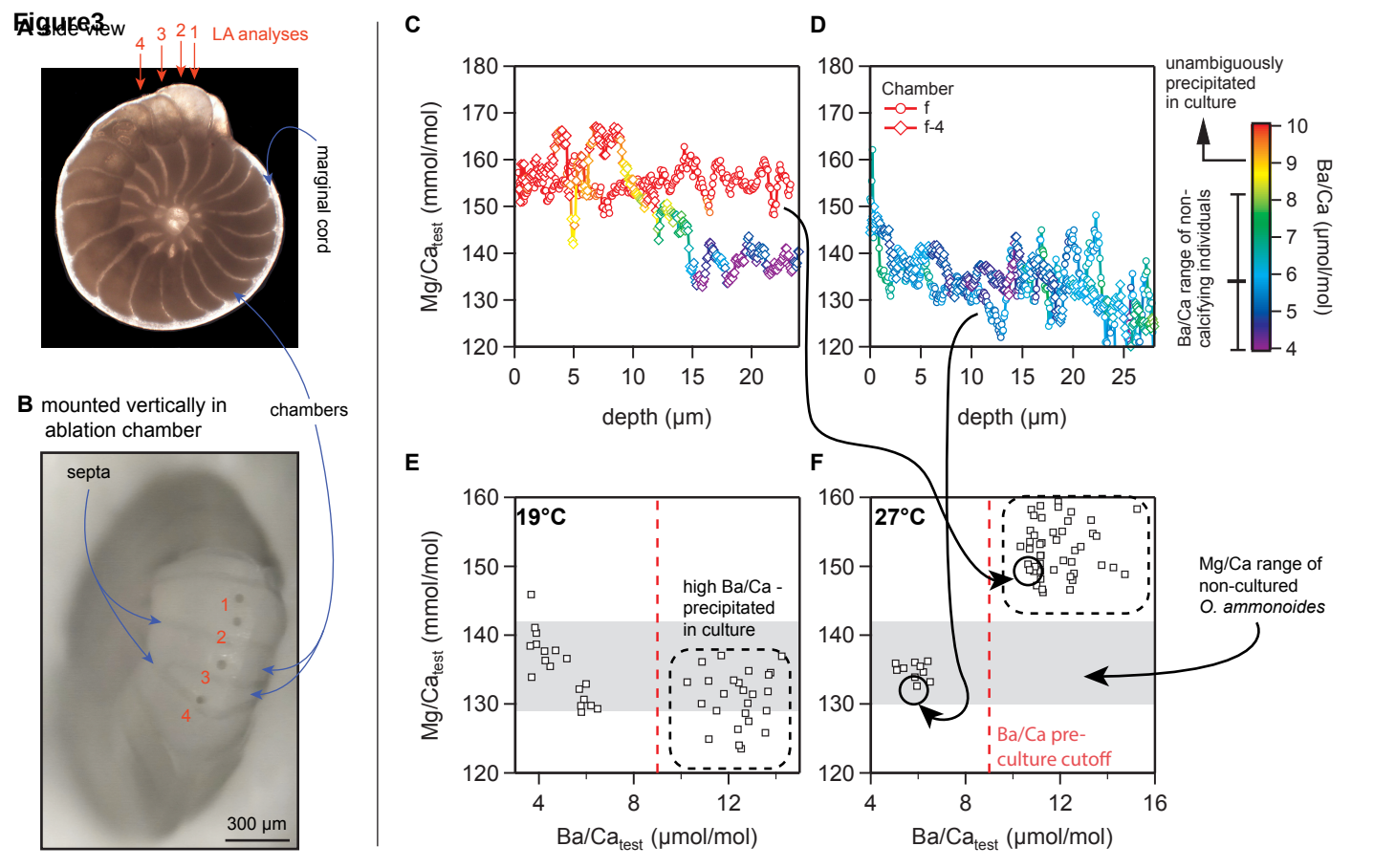
Figure3
A Side view
4
3
2
1
LA analyses
marginal cord
chambers
B mounted vertically in ablation chamber
septa
1
2
3
4
300 µm
C
D
Mg/Ca$_{test}$ (mmol/mol)
depth (µm)
Chamber
f
f-4
unambiguously precipitated in culture
Ba/Ca range of non-calcifying individuals
Ba/Ca (µmol/mol)
E
F
19°C
27°C
high Ba/Ca - precipitated in culture
Ba/Ca pre-culture cutoff
Mg/Ca range of non-cultured *O. ammonoides*
Ba/Ca$_{test}$ (µmol/mol)

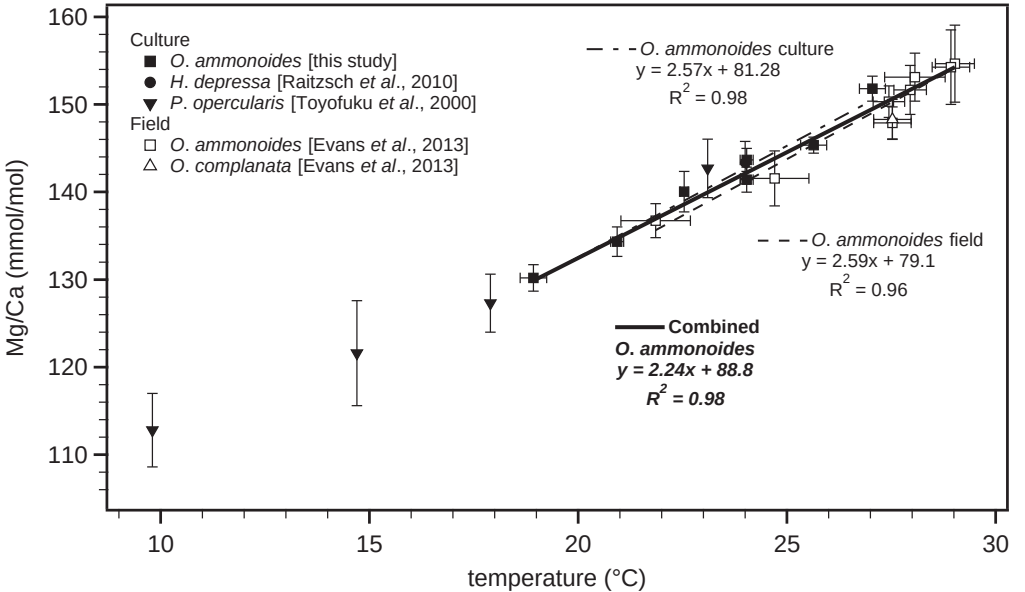
Culture
O. ammonoides [this study]
H. depressa [Raitzsch et al., 2010]
P. opercularis [Toyofuku et al., 2000]
Field
O. ammonoides [Evans et al., 2013]
O. complanata [Evans et al., 2013]
O. ammonoides culture
y = 2.57x + 81.28
R2 = 0.98
O. ammonoides field
y = 2.59x + 79.1
R2 = 0.96
Combined
O. ammonoides
y = 2.24x + 88.8
R2 = 0.98
Mg/Ca (mmol/mol)
temperature (°C)
160
150
140
130
120
110
10
15
20
25
30

Figure5

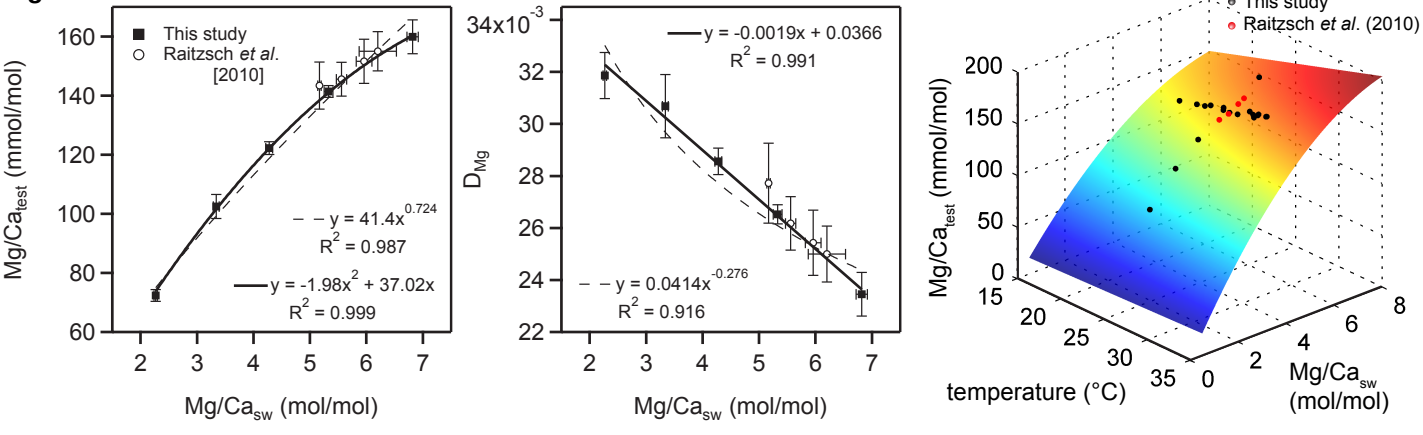
A
This study
Raitzsch et al. [2010]
y = 41.4x^0.724
R^2 = 0.987
y = -1.98x^2 + 37.02x
R^2 = 0.999
Mg/Ca_test (mmol/mol)
Mg/Ca_sw (mol/mol)
B
34x10^-3
y = -0.0019x + 0.0366
R^2 = 0.991
y = 0.0414x^-0.276
R^2 = 0.916
D_Mg
Mg/Ca_sw (mol/mol)
C
This study
Raitzsch et al. (2010)
Mg/Ca_test (mmol/mol)
temperature (°C)
Mg/Ca_sw (mol/mol)

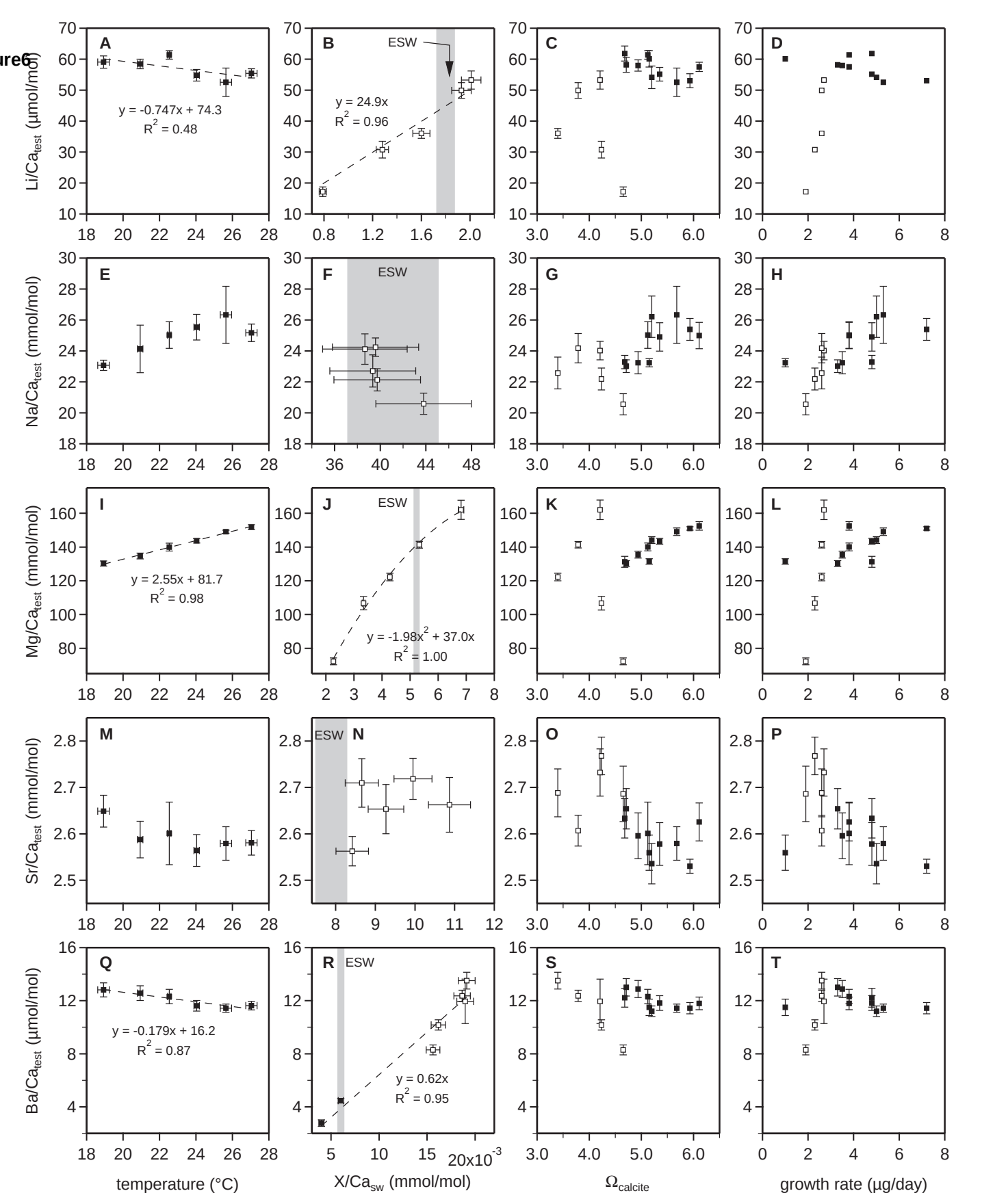
A
B
ESW
C
D
E
F
ESW
G
H
I
J
ESW
K
L
M
ESW
N
O
P
Q
R
ESW
S
T
Li/Ca$_{test}$ (µmol/mol)
Na/Ca$_{test}$ (mmol/mol)
Mg/Ca$_{test}$ (mmol/mol)
Sr/Ca$_{test}$ (mmol/mol)
Ba/Ca$_{test}$ (µmol/mol)
y = -0.747x + 74.3
R$^2$ = 0.48
y = 24.9x
R$^2$ = 0.96
y = 2.55x + 81.7
R$^2$ = 0.98
y = -1.98x$^2$ + 37.0x
R$^2$ = 1.00
y = -0.179x + 16.2
R$^2$ = 0.87
y = 0.62x
R$^2$ = 0.95
20x10$^{-3}$
temperature (°C)
X/Ca$_{sw}$ (mmol/mol)
Ω$_{calcite}$
growth rate (µg/day)

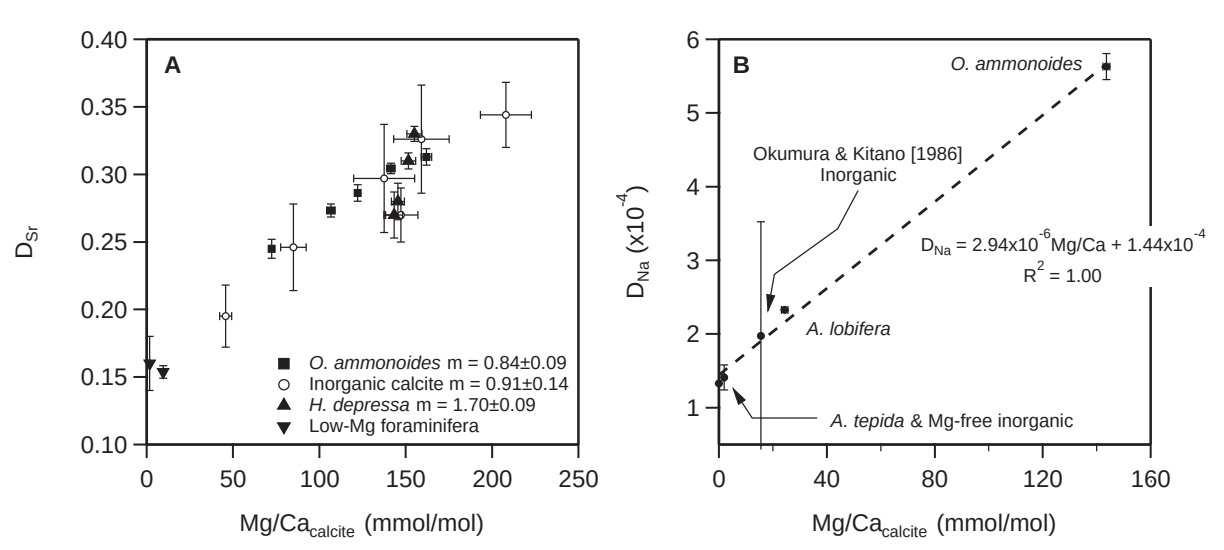
A
B
D_Sr
D_Na (x10^-4)
Mg/Ca_calcite (mmol/mol)
Mg/Ca_calcite (mmol/mol)
O. ammonoides m = 0.84±0.09
Inorganic calcite m = 0.91±0.14
H. depressa m = 1.70±0.09
Low-Mg foraminifera
O. ammonoides
Okumura & Kitano [1986]
Inorganic
D_Na = 2.94x10^-6 Mg/Ca + 1.44x10^-4
R^2 = 1.00
A. lobifera
A. tepida & Mg-free inorganic

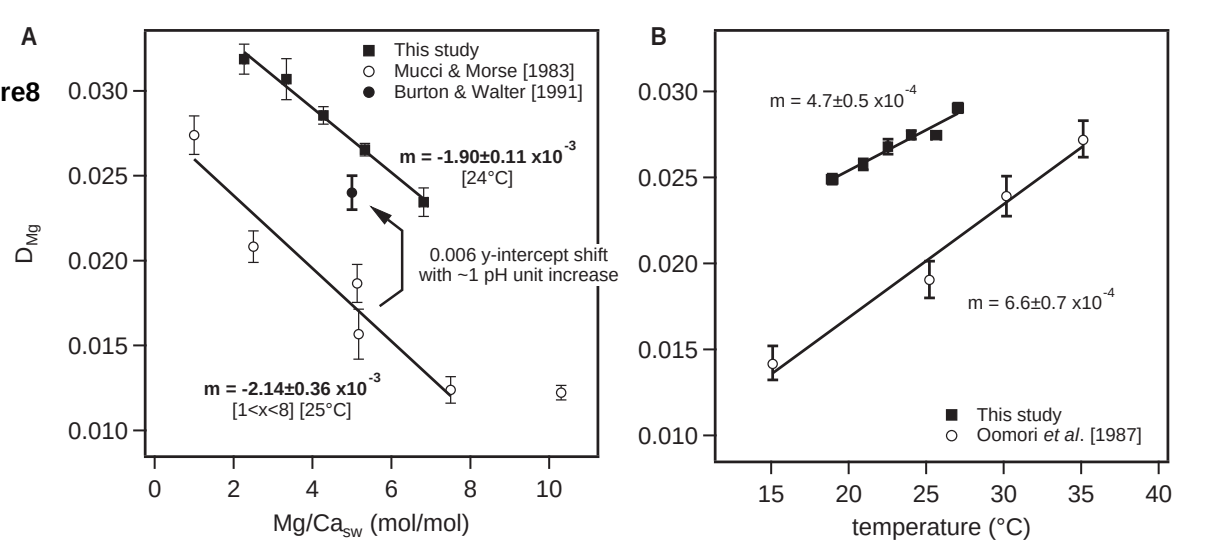
A
B
This study
Mucci & Morse [1983]
Burton & Walter [1991]
m = -1.90±0.11 x10-3
[24°C]
0.006 y-intercept shift
with ~1 pH unit increase
m = -2.14±0.36 x10-3
[1<x<8] [25°C]
DMg
Mg/Casw (mol/mol)
m = 4.7±0.5 x10-4
m = 6.6±0.7 x10-4
This study
Oomori et al. [1987]
temperature (°C)

**Electronic Annex**

**Click here to download Electronic Annex: Evans_et_al_SM.pdf**

**LaTeX Source Files**

**Click here to download LaTeX Source Files: OpCultGCAnoBibtex.tex**